



JIMMA UNIVERSITY

JIMMA INSTITUTE OF TECHNOLOGY

FACULTY OF MECHANICAL ENGINEERING

SUSTAINABLE ENERGY ENGINEERING MASTERS PROGRAM

DESIGN MODIFICATION, CFD MODELING, FABRICATION AND EXPERIMENTAL VALIDATION OF CONTINUOUS FEEDING BIOCHAR PRODUCING STOVE

A Thesis submitted to the School of Graduate Studies of Jimma University Institute of Technology in partial fulfillment of the requirements for the Degree of Master of Science in Sustainable Energy Engineering

By: Mamo Tesema

Advisor: Prof. Dr. A. Venkata Ramayya

Co-Advisor: Dr.-Ing. Getachew Shunki (PhD)

November, 2016

Jimma, Ethiopia

I, the undersigned, declare that this thesis is my original work and has not been presented for a degree in any University, and that all the source of materials used for the thesis has been duly acknowledged.

Declared by: Name: Mamo Tesemma

Signature: _____

Date: _____

Confirmed by: Name:

Signature: _____

Date: _____

ACKNOWLEDGEMENT

It is my pleasant duty to acknowledge grateful and generous who help me directly or indirectly, at all the stages of doing my thesis.

Firstly I would like to thank the Almighty God, then secondly I would like to grateful thanks for my advisors Prof. Venkata Ramaya and Dr.eng.Getachow Shunki (PhD) for giving their knowledge and their time and give me their precious advice at all stages of my work and about a report certainly to give sincere guidance, comments and constructive criticism. I thanks Mr. Yohanis Mitiku heartily, who shared me his experience and finding the research problem and taught me never to give up in spite of the circumstances; My thanks extend to Mr. Mitiku Soboka, who had been engaged in the manufacturing and development.

My special thanks go to Debela Geneti and Tarekegn Limore; for their encouragement, patience and support towards my academic career. At the end, I greatly acknowledge all persons earnestly with my heart.

Contents

ACKNOWLEDGEMENT	iii
EXECUTIVE SUMMARY	x
CHAPTER ONE	1
1. INTRODUCTION	1
1.1 Back Ground	1
1.1.1 Ethiopia and its Energy situation	2
1.1.2 Improved cook stoves in Ethiopia.....	4
1.2 Motivation.....	5
1.3 Statement of Problem.....	6
1.4 Objective	7
1.4.1 General objective	7
1.4.2 Specific objectives	7
CHAPTER TWO	8
2 LITERATURE REVIEW	8
2.1 Global potential of cookstove	8
2.2 Cook Stove development in Ethiopia.....	8
2.3 History of biochar producing cookstoves for multipurpose.....	9
2.4 Benefits of biochar cook stoves	10
2.5 Biochar cookstove design basis	10
2.5.1 Direct Combustion Stove	11
2.5.2 Indirect Combustion.....	12
2.7 Stove descriptions	15
2.8 Pyrolysis Process Types.....	15
2.8.1 Fast Pyrolysis	15
2.8.2 Slow Pyrolysis	16
2.9 Biochar production and its pH value.....	16
2.11 Chemical and physical Characteristics of Biochar.....	17
2.12 Impact of Biochar Applications on Soil Quality and Crop Productivity	18
2.13 Using Biochar for carbon Sequestration in soil	20
2.14 Recommendation by Past Researchers	23
2.15 Research gaps still to be addressed	23
2.16 Scope of the research	24

CHAPTER THREE	25
3. RESEARCH METHODOLOGY AND DESIGN BASIS	25
3.1 Materials	25
3.1.1 Description of the Study Area:.....	25
3.1.2 Material Used for the Experimental Test fabrication.....	25
3.2.1 Computational fluid dynamics analysis	27
3.2.2 Construction	32
3.2.3 Experimental validation	33
CHAPTER FOUR.....	53
4. RESULTS AND DISCUSSION	53
4.1 Simulation results.....	53
4.1.1 Transient heat transferred through the stove and biochar	53
4.2 Results from experimental validations.....	58
4.2.1 Water boiling test.....	58
4.2.2 Produced Biochar and its characterizations	63
4.3 Comparison of CFD simulation results and Experimental data.....	68
Conclusion	70
Recommendations.....	71
Bibliography	73
Appendixes	78

List of figures

Figure 1: The primary source and energy consumption of fuel used in Ethiopia.....	2
Figure 2: Wood-stove commonly used in rural Ethiopia.....	9
Figure 3: Relationship between pyrolysis temperature and the C concentration of the resulting biochar..	18
Figure 4: Schematic of biochar solution	19
Figure 5: Functions of biochar.....	20
Figure 6: The biochar Carbon cycle.....	21
Figure 7 : 3D geometry of the stove	28
Figure 8: Mesh geometry	29
Figure 10: Constricting the continuous feeding biochar producing stove	33
Figure 11: Normal Anila stove.....	34
Figure 12: Continuous feeding anila type stove.....	34
Figure 13: Sample of water boiling test and measuring temperature for the selected stoves	36
Figure 14: Transient heat transfer throughout the stove at different time from bottom to top	53
Figure 15: Transient heat transfer through the biomass to be charred.....	54
Figure 16: Effect of mesh size	54
Figure 17: Effect of primary air flow direction.....	55
Figure 18: Folw velocity in the combustion chamber of stove.....	55
Figure 19: Trend of Temperature with time in coffee husk at selected point	56
Figure 20: Heat transfer throughout the biochar from bottom to top at (45min).....	56
Figure 21: Temperature variation throughout the stove at 45min from bottom to top	57
Figure 22: CFD results of temperature variations within biomass to be charred at selected line from inner to outer at 45min	57
Figure 24: Experimental results which shows the effect of secondary air inlet.....	58
Figure 25: Temperature versus time at different position of stoves for coffee husk	59
Figure 26: Experimental Temperature variations with position for selected stoves at 60min	59
Figure 27: Average time of cooking processes (coffee husk).....	60
Figure 28: Average fuel consumption for all stove.....	61
Figure 29: Thermal efficiency of the three stoves in the case of high power and low power test	61
Figure 30: Comparison of the power of the each stoves.....	62
Figure 31: Comparison of turn down ratio of each stoves	63
Figure 32: The biochar produced from the three types of stove	64
Figure 33: Biomass mass loss (%) to biochar versus time (min).....	65
Figure 34: Biochar yield of selected biomass at different temperature (K)	66
Figure 35: Surface area of biochar produced in new stove at different temperature	67
Figure 36: Experimental and CFD simulation result of temperature variation with time for selected point	68
Figure 37: Experimental and Simulation result of Temperature variation with position.....	69

List of table

Table 1: Estimated fuel wood demand and supply balance for Ethiopia (in million m³) [13] ----- 3
Table 2: CFD applications in biomass gasification and pyrolysis [15, 16, 17, 18, 19, 22]----- 14
Table 3: Indirect stove descriptions [42, 18, 27, 24]----- 15
Table 4: Proximate analysis of biochar gained from selected biomass----- 65
Table 5: pH of biochar produced of continues feeding biochar producing cook stove by experiments --- 67

Nomenclature

0.1NHCl 0.1	Normal hydrochloric acid
0.1NNaOH 0.1	Normal sodium hydroxide
A	Surface Area
ANOVA	Analysis of Variance
ASTM	American society Testing and material
BD	Bulk density
C	Carbon
°C	Degree centigrade
CEC	Cation exchange capacity
CFD	Computational Fluid Dynamics
CFAT	Continuous feeding Anila type stove
CFBP	Continuous feeding biochar producing stove
CH ₄	Methane
CO	Carbon Monoxide
EHV	Effective Calorific Value
GDP	Gross domestic product
GHG	Greenhouse Gas
gm	Gram
h	Hour
HHV	Gross Calorific Value
ICS	Improved cooking stoves

LHV	Net Calorific Value
m ²	Square meter
m ³	Meter cube
mg	Milligram
ml	Milliliter
M _o	Moisture is considered for fuel
M _t	Metric tons
N	Nitrogen
NaCl	Sodium chloride
T	Temperature
T LUD	Top-lit updraft gasifier
UDF	User defined Function
V	Volume
W BT	Water Boiling test

EXECUTIVE SUMMARY

Household energy use and biochar in developing countries like Ethiopia have gained a tremendous interest in the past decade. The adoption of a simple household pyrolytic stove has the potential to provide multiple benefits from reducing the rate of deforestation, improved soil fertility, enhanced household air quality to mitigating climate change. The Green Solution Concept focuses on using biomass waste resources. The main objective of this study is Design optimization, CFD simulation, fabrication and experimental validation of continuous feeding biochar producing cook stove. Overall, approximately 45 cases were studied during the development of this model. The majority of these cases were run to gain an understanding of how various parameters affected the solution. This paper summarized the CFD applications in biomass combustion and system design. There is evident that CFD can be used as a powerful tool to predict biomass combustion and heat transfer processes as well as to design combustion chamber or reactor.

CFD has played an active part in system design including analysis the flow, and temperature. During the course of this research project, realistic geometry, flow conditions, and fuel properties were incorporated into a 3D numerical model using Fluent CFD software (ANSYS 14.5). By performing simulations with different direction of air inlet and mesh size, it was shown that the 3D model performed fairly well, and exhibited the expected trends for temperature, and flow gases. Similar with CFD simulation, experimental results shows the temperature variation within biomass bed is high in both NA and CFAT stoves while it is small temperature variation in CFBP stove. Thermal efficiency was performed on the three selected stoves using eucalyptus tree as a fuel. It was observed that the CFBP cook stove, CFAT stove and NA stove shows a thermal efficiency of 25%, 18%, and 17% in the case of high power test (cold start). and also the thermal efficiency of CFBP stove, CFAT stove and NA stove shows 15%, 13%, and 13% in the case of low power test (simmering) Thus, it was found that the thermal efficiency of CFBP cook stove is found to be higher when compared with the other two pyrolytic stoves in both cases.

The biochar produced is highly alkaline, with all pH values recorded above pH 9.33 to a maximum pH of 9.63. The variability within the sample chosen from each burn is low, which means that coffee husk biochar produced experimentally is consistent in terms of pH with in a given burn.

Jimma University, Jimma institute of Technology, Faculty of Mechanical Engineering, Sustainable Energy Engineering program

CHAPTER ONE

1. INTRODUCTION

1.1 Back Ground

A growing energy demand, in combination with a changing climate and the dwindling natural resources, is one of the major challenges facing the world today. About 3.5 billion people in the world rely on the traditional use of biomass, mostly firewood, for cooking. In many areas this implies pressure is put on the forest resources. Using wood energy for cooking may also bring a health risk, due to exposure to smoke. Every year, 3.5 million people die prematurely as a result of respiratory diseases caused by smoke inhalation related to these cooking methods. [1]

Internationally, access to renewable energy is becoming an increasingly important topic, as expressed in for example the designation of 2012 as the International Year of Sustainable Energy for All by the United Nations General Assembly and the process of climate negotiations. Although improved cooking stoves (ICS) have been promoted for decades, the renewed international attention stresses the importance of these stoves as low-cost solution to improve indoor air quality, help reduce greenhouse gases, relieve the daily workload of women and reduce expenditure on energy in poor households [2].

Rural populations are heavily relied on the biomass to satisfy their daily needs. Due to higher energy content and abundant availability, agricultural solid biomass waste offer great potential as a fuel, which is used in traditional and pyrolytic cook stoves as an alternate for fossil fuels. However, incomplete combustion of solid fuels in low efficiency traditional cook-stove tends to emit hazardous pollutants such as GHGs, CO, CH₄ and polycyclic aromatic hydrocarbons (PAHs) etc. [1] and there by affect human health causing respiratory problems and other health issues.

Improving the energy efficiency of biomass burning stoves potentially offers a highly cost-effective alternative for easing the burden of buying fuel by urban poor and collecting fuel by rural poor. Better stoves also promise important health benefits to their users by reducing smoke emissions. Almost all African countries still rely on wood to meet basic energy need. Wood fuels

Jimma University, Jimma institute of Technology, Faculty of Mechanical Engineering, Sustainable Energy Engineering program

account for 90-98% of residential energy consumption in most sub-Saharan Africa [3]. Like many other sub-Saharan African countries, Ethiopia is highly dependent on biomass energy sources, such as fuel wood, charcoal, animal dung and crop residues [4].

1.1.1 Ethiopia and its Energy situation

Excluding human and animal energy, the sources of energy supply in Ethiopia can be classified into traditional and modern energy. Traditional sources include wood fuel, agricultural residue, and charcoal and cattle dung collectively known as biomass. It accounts to about 95.8% of the total energy supply of the country [5]. Modern energy consists of electricity and petroleum products, and accounts to the remaining 4.2% of the national energy supply sources. From the total modern energy supply, on average, petroleum constitutes 86% and the remaining 14% is derived from electricity, of which 96.7% is from hydro and 3.3% from diesel generators [6].

From the national energy consumption the share household sector, is more than 88%, Service is 3%, Industrial is 5%, Transport is 3% and Agriculture is 1%. Out of this share, rural households account for about 92% of the total household consumption [7]. The supply of fuel wood is diminished from time to time with population growth. This led to the rural population to spend a large percentage of their time searching for fuel wood instead of performing productive work in agriculture.

These biomass energy sources account for more than 90% of total domestic energy demand, according to the Ethiopian Environmental Protection Agency

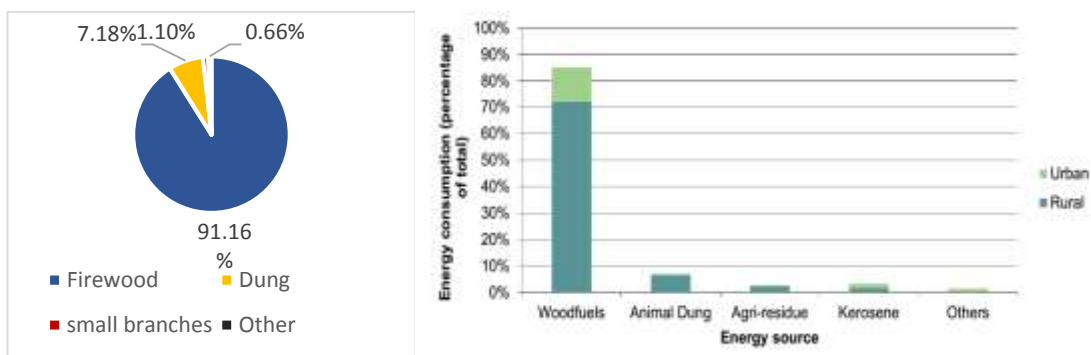


Figure1: The primary source and energy consumption of fuel used in Ethiopia [7].

Fuel wood scarcity has led to a growing dependence on crop residues and animal dung as fuel, which otherwise would have been used as animal fodder and for the restoration of soil fertility. This could potentially lead to severe reduction in agricultural output at a time when greater production is expected in the sector. Similarly, shortages and high costs of fuel wood lead to the reduction in the number of cooked meals, especially by the urban poor who cannot afford to switch to modern fuels. This would have adverse health effects.

In Ethiopia, it is identified that biomass energy usage is a key issue in the national economy in general and the energy sector in particular. The underlying reason is that the cooking and baking is the major consumer of energy, and almost the entire energy demand of this sub-sector is met from a biomass resource. In many parts of the country, unsustainable exploitation of biomass resources has resulted in adverse economic and environmental impacts. Most of the resources (finance, labor and time) are over extended due to the rising prices of fuel and an ever increasing distance of fuel wood collection sites.

Though, it could be at different magnitude, all regions in Ethiopia are in short of biomass energy supply to meet their current level of demand. The fuel wood demand and supply projection and analysis made by the Ethiopian Forestry Action Program in 1996 showed that in the year 20012 the demand for fuel wood was estimated to be 58.4 million m³ while the sustainable supply is only 11.2 million m³ making the deficit to 47.1million m³. For the Year 2014, these figures are projected to be 88.9, 8.8 & 80 million m³ in the above order (table 1.1)

Table 1: Estimated fuel wood demand and supply balance for Ethiopia (in million m³) [13]

Year	Demand	Supply	Deficit
1997	52.9	11.7	41.2
2000	58.4	11.2	47.2
2005	68.5	10.4	58.1
2014	88.9	8.8	80

The impact on crop production is also another problem. When the demand for biomass energy exceeds the available supply of wood fuel, increasing quantities of cow dung and agricultural residues used for energy, otherwise could have been used to enhance crop production. Dung contains 1.465% elemental nitrogen and 1.30% elemental phosphorous of oven dry weight.

One tone of urea contains the nitrogen equivalent of 32 tons of dry manure. Dominium phosphate contains both nutrients in proportions roughly equivalent to dry cow dung. Its composition is 21% nitrogen and 23% phosphorous (44% in total). One tone of Dominium phosphate roughly equals 16 tons of dry dung. This assessment obviously excludes various other nutrients contained in dung, which can contribute to plant growth [14][5].

1.1.2 Improved cook stoves in Ethiopia

Cooking is the largest energy consuming end use in Ethiopia. More than 80% of the total energy supplied in the country goes to meeting cooking requirements in the social, commercial and residential sectors[7]. In all sectors, cooking is done mostly with non-renewable biomass fuels using stoves of very low efficiency practically all Ethiopian households use wood fuels for cooking. Commercial and social institutions such as bakeries, restaurants, schools, detention centers, universities and hospitals also use wood to cook[8].

As a result the total amount of wood consumed for cooking, estimated at some 62 million tons annually, makes up more than 80% of the total energy consumed in the country and puts huge pressure on natural resource sustainability.

1.1.3 CFD modeling principles

Due to a combination of increased computer efficacy and advanced numerical techniques, the numerical simulation techniques such as CFD became a reality and offer an effective means of quantifying the physical and chemical process in the biomass thermochemical reactors under various operating conditions within a virtual environment. The resulting accurate simulations can help to optimize the system design and operation and understand the dynamic process inside the reactors.

CFD modeling techniques are becoming widespread in the biomass thermochemical conversion area. Researchers have been using CFD to simulate and analyze the performance of thermochemical conversion equipment such as fluidized beds, fixed beds, combustion furnaces, firing boilers, rotating

cones and rotary kilns. CFD programs predict not only fluid flow behavior, but also heat and mass transfer, chemical reactions (e.g. devolatilization, combustion), phase changes (e.g. vapor in drying, melting in slagging), and mechanical movement (e.g. rotating cone reactor). Compared to the experimental data, CFD model results are capable of predicting qualitative information and in many cases accurate quantitative information.

CFD modeling has established itself as a powerful tool for the development of new ideas and technologies. The complex structure makes biomass compositions pyrolyze or degrade at different rates by different mechanisms and affect each other during thermochemical process, and it makes the biomass particle feedstock has anisotropic properties in physical characterization [1].

How to deal with or simplify the complex process is a key point for the CFD simulation model. Many studies have been done on the biomass pyrolysis kinetics and the transfer and tracking of the feedstock particles, which have applied to CFD modeling and made good achievements. Simulations on reactor design, pyrolysis process, combustion systems, and particle deposit and pollutant release have been performed with CFD packages. In this paper, we attempt to summarize the current state of various CFD applications concerning the biomass thermochemical conversion process. The challenges faced by modelers using CFD in the biomass pyrolysis are also discussed.

Computational fluid dynamics is a design and analysis tool that uses computers to simulate fluid flow, heat and mass transfer, chemical reactions, solid and fluid interaction and other related phenomena. Comparing to the physical experiment operation, CFD modeling is cost saving, timely, safe and easy to scale-up

1.2 Motivation

The main motivators for use of pyrolytic stoves in developing countries.

- ✓ Simulation of heat transfer through the biochar producing stove by CFD software
- ✓ Fabricating multi-purpose of cook stove for Biochar production and extracting energy from biomass while cooking meal.
- ✓ Reducing the overall weight of the stove and supplying uniform heat to the biomass to be charred from inner cylinder and outer cylinder is also my career goal.

1.3 Statement of Problem

Emissions from solid fuel combustion to indoor, regional and global air emission inventory largely depend on fuel types, combustion devices and other factors. The use of biomass cook stove is widespread in the domestic sector of developing countries like Ethiopia, but these stoves are not efficient and generate high amount of GHG emissions.

Approximately half of the world population and up to 90% of rural households in developing countries still rely on biomass fuels and use conventional three stone stove to prepare their meals. Due to improper design of combustion zone and low thermal efficiency, it emits gaseous pollutants like CO, particulate matter, etc.

- Firstly, the pyrolysis stove would take too long of a time for the secondary fuel to begin gasifying and the stove was therefore an inefficient version of the wood stove for the largest part of the burn time, moreover, the stove worked on
- Another problem of using the pyrolysis stove was safety. The outer cylinder is very hot after the pyrolysis has started, and can cause burn injuries. Special concern were the kids, who possibly play around and could accidentally fall on the stove.
- The lifting issue was also raised. The empty model stove weights approximately 6 kg. However, the stove must be filled first with biomass, and then turned around. The estimated weight for the biomass is approximately 3kg. Also to adjust the ring to hold the bottom tightly closed, requires some amount of force [9].
- The stove worked on a batch system, in that the stove needed to be loaded once before its use and filling it with biomass and then would have to wait until the end of its use and for it to cool, before you could remove the biomass and reload

1.4 Objective

1.4.1 General objective

The general objective of this thesis is Design modification, CFD simulation, fabrication and experimental validation of continuous feeding biochar producing cook stove.

1.4.2 Specific objectives

The specific objective of present research is to study a detailed scientific understanding of heat transfer as it relates to the design of biomass cook stoves. If heat transfer between the pot surface and hot gases from the fire is optimized, and then overall thermal efficiency of the cooking operation can be improved significantly. Achieving this through cost effective means allows more people in developing countries to reduce their health burden and reduce the environmental impacts significantly.

In order to minimize the losses to the surroundings and maximize the transfer of heat to the food in the pot, a thorough knowledge of heat transfer mechanisms and their underlying principles is required to determine the reasons for the losses, how these losses can be reduced through modifications of the design of the cook stove etc.

There are four specific objectives, which the research encompasses.

- To improve the heat transfer in the combustion chamber by CFD modeling and analytical modeling.
- Fabricate the stove and do the experimental testing to evaluate performance of the stove by WBT version 4.2.2
- Characterizing the produced biochar during WBT.

CHAPTER TWO

2 LITERATURE REVIEW

2.1 Global potential of cookstove

The global energy consumption was about 16408.5 MTOE in the year 2014 of which 11% of the energy is derived from biomass [10]. Wood contributes to about 50% of energy derived from biomass. Biomass is used as fuel mostly in rural area for cooking. A household using traditional cook stoves consumes about 1800kg of fuel wood every year for cooking. Thus by using improved cook stoves the fuel consumption can be reduced by 40% to 60% thereby retarding the deforestation rate and global warming potential of greenhouse gases emitted by combustion of this biomass.

Domestic cooking makes up a major portion of the total energy used in developing nations, close to 60% in Sub-Saharan Africa, so that nearly 3.5 billion people worldwide cook their meals on simple stoves that use biomass fuels [11].

2.2 Cook Stove development in Ethiopia

Biomass is an important energy source in Ethiopia. Biomass energy represents about 94% of total energy consumption. About 89% of the biomass energy supply is used by households. Given the low level of efficiency attained by traditional biomass technology used in the Ethiopian households, improving domestic cooking efficiency has been given emphasis.

Cooking efficiency improvement has been carried out in Ethiopia by government and NGO's. Since the 1970s the EREDPC, has been engaged in the business of improving household cooking efficiency, resulting in two improved cook stoves, namely: "Laketch" charcoal stove, and the "Gonzie" multi-purpose wood stove used for baking, cooking and boiling.[2]



Figure 1: Wood-stove commonly used in rural Ethiopia [12]

The “Laketch” charcoal stove has an efficiency of 19 – 21% and a fuel saving of 25% compared with traditional stoves. The stove is popular among urban dwellers and is used mostly for coffee making and cooking stew. To date over 2.5million stoves have been disseminated [9].

There are also different types of metal charcoal stoves of different sizes in the market square, funnel and circular shapes. The most widely used are the square and funnel shaped stoves. These stoves are taken as traditional charcoal stoves. The Grates of the metal charcoal stoves are removable.

2.3 History of biochar producing cookstoves for multipurpose

The most common method of cooking used in developing countries is an open fire. The fire is usually shielded or surrounded by “three or more stones, bricks, mounds of mud, or lumps of other incombustible material” [13]. The three-stone fires have continued to be used for cooking and heating purposes, mainly due to their simplicity. They are easy to build and virtually free. They can be adapted to different forms quite easily – i.e. placed on waist-high platforms for more convenience for the user. There are more sophisticated types of traditional stoves, ranging from mud stoves to heavy brick stoves to metal ones. Most sources cite the fuel-efficiency of traditional stoves as 5% – 10% [14].

Pyrolysis stoves are able to cleanly harvest the energy contained in low grade organic waste or bio-residues, which means they use less wood than traditional stoves [15]. Such a biochar system could be said to supply energy without fossil fuels, reduce deforestation and also the likelihood

Jimma University, Jimma institute of Technology, Faculty of Mechanical Engineering, Sustainable Energy Engineering program

of land conversion by improving crop yields-combatting the three main causes of climate change.

In order for biochar stoves to become an effective environmental strategy, their role in supplying energy, reducing pressure on deforestation and biochar production must be carefully examined. The energetic aspects of stoves have been studied since the late 1970s and are generally well understood, but there has been little- if any – research into the biochar produced by stoves. This is because they are recent invention, but also because the nature of the biochar has possibly not even registered concern among stove developers. Biochar has a high calorific value, so its production inevitably reduces the potential benefit to soils.

As biochar production is a subsidiary aim of pyrolysis stove design, this means that the pyrolysis conditions have been optimised for cooking, rather than supplying a biochar of a consistent nature. This presents concerns within the context of soil application; if the properties of biochar that are added to the same soil vary significantly, its effect on soil fertility will be similarly unpredictable. Further to this, the feed stocks that will be used in pyrolysis stoves (agricultural waste and bio-residues) produce biochars with properties different to that of wood which currently represents the majority of all feed stocks used for biochar soil application.

2.4 Benefits of biochar cook stoves

The benefits associated with biochar producing cook stove fall in two categories: those that are internal to the household and those that are external. Internal benefits include: reduced concentrations of smoke and indoor air pollution; money and time saved in acquiring fuel; and reduced biomass use, ability use animal dung as fertilizer instead of for fuel. External benefits include: less pressure on forest and energy resources; reduced GHG; and skill development and job creation in the community [21].

2.5 Biochar cookstove design basis

There are two basic stove operations in the production of biochar. The first type of stove produces biochar by direct combustion of biomass. The second type involves burning the biomass in one chamber and housing the biomass to be charred in the annular portion of an outer

chamber. Heat is transferred from the burning fuel on the inner chamber to the material to be charred in the outer chamber.

2.5.1 Direct Combustion Stove

Here biomass is burnt inside a cylinder in an oxygen limited environment. The biomass goes through a gasification cycle where most of the volatile components are released and flared. The resulting residue is the bio-char. Top lit up draft gasifier [TLUD] is a popular version of this type. Prototype of the TLUD was built based on the basic principles of an inner cylinder forming the combustion chamber within an outer cylinder for regulating primary and secondary air flows [13]. The TLUD (Top Lit Upward Draft) gasifier was originally designed by Paal Wendelbo which he took to Africa in 1988. Since then, the design has been adapted and distributed around the world. A prototype of the design amended by Anderson has been produced and tested in Cambodia. A model was also adapted by ARTI in India [16]

The basic sizing calculations involve determining the stove diameter and height for a desired biochar burning rate. The chemical composition of the biochar is required based on which the stoichiometric air and resulting flue gas flow rate can be calculated. Sizing calculations are made based on basic thermodynamics and chimney stack draught flow principles. The required air flow for pyrolysis is kept just below stoichiometric air requirement. The total air flow is divided into primary and secondary air flows in the ratio of 9:1. The diameter of the stove (D) is fixed to give a maximum gas velocity 1m/s. The calculations for stack height are made to achieve the natural draught to drive the process of pyrolysis

$$q = CA \sqrt{2gH \frac{T_i - T_e}{T_e}} \quad (2.1)$$

Where: q = flue gas flow rate (m³/s),

A = cross sectional area (m²),

C = discharge coefficient,

G=gravitational acceleration (m/s²),

H = height of chimney (m),

T_i = average temperature inside chamber (K),

T_e = external temperature (K).

The discharge coefficient is based on the discharge coefficient for subsonic flow through a round orifice (0.6 to 0.65). The average temperature inside the chamber is the average temperature of flue gas during combustion. The height of the stove is determined based on the rate of natural draught by the stack height and is decided by the relation given in Equation (1)

2.5.2 Indirect Combustion

Here the biomass is burned in the inner chamber and the biomass to be charred is housed in the annular portion between the inner chamber and outer chamber. Heat is transferred from the burning fuel on the inner cylinder to the material to be charred in the outer cylinder. Airflow can be based on natural draught or through a separate fan [17].

The stove under discussion is provided with a fan. The rocket stove is developed by Larry Winiskari. It is simple in design. The rocket stove is very efficient in that it is clean and produces no smoke. It allows for the heat to be concentrated in thermal mass. Heat can be directed to a central point as with the other biochar stoves, and allows for the smoke produced by pyrolysis and gasification to be burned, thus eliminating the exhaust of smoke fumes from the stove.

The heat required to dry the biomass in the retort and turn it to biochar is given by Equation (2).

$$Q_{bio} = (2.5 \times m_{bio} \times M) + (2.5 \times m_{bio} \times (9H_2)) \quad (2.2)$$

m_{bio} = mass of biomass to be charred, M = moisture equation in biomass/kg, H_2 = hydrogen in biomass/kg, 2.5 = heat required to evaporate moisture in MJ/kg. The heat obtained by burning of the biomass is given by Equation (3).

$$Q = m_f \times HV \quad (2.3)$$

The heat obtained by burning of the biomass should be sufficient to dry the biomass in the retort and turn it to biochar. This determines the mass of biomass to be burned. The heat obtained by

Jimma University, Jimma institute of Technology, Faculty of Mechanical Engineering, Sustainable Energy Engineering program

burning the biomass is transferred to the biomass to be charred through the wall of the inner chamber by conduction. This fact is used in determining the dimensions of the stove like height and diameter. Heat transferred by conduction through the wall = Q_{cond} and is given by Equation (2.4).

$$Q_{cond} = Q_{bio} \tag{2.4}$$

$$Q_{cond} = \frac{2\pi k H (T_i - T_o)}{\ln\left(\frac{r_o}{r_i}\right)}$$

Where, k = thermal conductivity of material of stove,

H = height of stove,

r_o = outer radius of inner chamber

r_i = inner radius of inner chamber,

T_i = inside temperature = combustion temperature,

T_o = outside temperature = charring temperature.

T_i can be taken as 1800°C and T_o can be taken as 500°C as a rough approximation [18]. The required air flow through inner chamber is kept just above stoichiometric air requirement. The diameter of the inner chamber is fixed to give a maximum velocity 1m/s as in the case of TULD stove. This fixes the inner radius of the inner chamber. The outer radius is fixed based on the thickness chosen. Using the heat transferred by conduction, the height of the stove can be fixed once the inner and outer radius of the inner chamber is fixed.

2.6 Applications of CFD in biomass gasification and pyrolysis

The CFD models used to describe these processes have become an important analysis and design tool to achieve the flow and temperature pattern, the products concentration contour and yields. [15] Developed a detailed CFD model to simulate the flow and reaction in an entrained flow biomass gasifier. The model is *Jimma University, Jimma institute of Technology, Faculty of Mechanical Engineering, Sustainable Energy Engineering program*

based on the CFX package and describes the phenomena of turbulent fluid flow, heat transfer, species transport, devolatilization, particle combustion, and gas phase chemical reactions. Biomass particulate is modeled via a Lagrangian approach as it enters the gasifier, releases its volatiles and finally undergoes gasification.

Table 2: CFD applications in biomass gasification and pyrolysis [15, 16, 17, 18, 19, 22]

Application	Code	Aim/Outcome	Turb. Model	Agreement with Exp.	Authors
Entrained flow gasifier	CFX4	Products mass fraction distribution; temperature contours; swirl velocity distribution	Std k ϵ RSM	Acceptable	Fletcher, D. F.
Two-stage downdraft gasifier	Fluent	To investigate in detail the oxidation zone; temperature profile; velocity pattern; tar conversion mechanism study	RNG k ϵ	Satisfactory	Gerun, L.
Horizontal entrained flow reactor	Fluent	Predictions of flow, temperature and conversion; sensitivity of the kinetic parameters of pulverized corn stalk fast pyrolysis	n/a	Reasonable	Xiu, S. N.
Cone calorimeter reactor	Code	To model heat transfer and pyrolysis within dry and wet wood specimens, and the mixing and pilot ignition of the released volatiles	n/a	n/a	Yuen, R. K. K.
Downdraft gasifier	Code	Temperature profile, pressure drop, model parametric analysis	n/a	Good	Luo, Z. Y.

2.7 Stove descriptions

Table 3: Indirect stove descriptions [42, 18, 27, 24]

Stoves	Developer	Design	Innovations/Notes
Anila	Dr. Ravikumar	True pyrolysis stove, Natural draft, Fed with agro waste	Pyrolysis chamber is separate from, surrounding combustion chamber. Pyrolysis gases are vented into combustion chamber. Stove retains heat long after the main combustion is extinguished
LUCIA, stove	By World stoves(Italy)	Pyrolyzing stove, natural-draft or fan-powered versions, batch fed, charcoal-producer	Highly modular design can be configured for gasification or pyrolytic operation. Complex flow path designed using CFD.
Continuous Anila	Mr Teka	Pyrolysis stove	Design of Continuous feeding fuel with CFD model of heat transfer through the stove.

2.8 Pyrolysis Process Types

There are two main classes of process for biomass pyrolysis, introduced briefly below

2.8.1 Fast Pyrolysis

Fast pyrolysis is characterized by high heating rates and short vapour residence times. This generally requires a feedstock prepared as small particle sizes and a design that removes the vapours quickly from the presence of the hot solids. There are a number of different reactor configurations that can achieve this including ablative systems, fluidized beds, stirred or moving beds and vacuum pyrolysis systems. A moderate (in pyrolysis terms) temperature of around 500°C is usually used.

2.8.2 Slow Pyrolysis

Slow pyrolysis can be divided into traditional charcoal making and more modern processes. It is characterised by slower heating rates, relatively long solid and vapour residence times and usually a lower temperature than fast pyrolysis, typically 400°C.

2.9 Biochar production and its pH value

Biochar is a solid material obtained from the carbonization of biomass. In recent years, scientific attention has been focused on its effect on soil amendment and ecological restoration. Biochar is added to improve the soil. Biochar can increase the soil fertility, increase agricultural productivity, and provide protection against some foliar and soil-borne diseases [19]. The technique of using charcoal as biochar was first developed in the Amazon basin over 2500 years ago as a means to improve soil fertility in the areas in which the indigenous inhabitants used to cultivate their crops. Biochar also has the potential to help mitigate climate change via carbon sequestration.

Currently the most common method of producing biochar is through biochar stoves. The basic process of producing biochar is by thermo chemical conversion. This includes the processes of gasification and pyrolysis. In pyrolysis, biomass is decomposed by secondarily heating it with controlled oxygen to support the combustion process of the biomass.

In the combustion of biomass, there are various stages and steps that take place before and after the burning. To evaporate the moisture content present in the biomass, it is heated up to approximately 100°C. In the range between 0°C - 100°C, no heat is generated from the burning of the biomass. The solids that are present in the biomass start to breakdown and convert to fuel gases as the temperature approaches 300°C. The main energy present in the fuel is released when the fuel vapours containing up to 60% of the energy burn at temperatures between 300°C - 600°C. After all the fuel vapours have been combusted biochar is left behind.[20]

The pyrolytic process converts biomass acids into the bio-oil component and the alkalinity is inherited by the solid biochar [21]. Inorganic carbonates and organic anions are alkaline components in biochar [22]. When biochar is produced at different temperatures, their alkalinity increases with increasing charring temperature [21].

When biochar with higher pH value was applied to the soil, the amended soil generally became less acidic [22]. The ameliorating effects of biochar on soil pH clearly increased with increasing biochar rates [23]. The improvement of crop growth from biochar amendment of a typical Ultisol may result from an increase of PH and cation exchange capacity (CEC) [24]. The pH of biochar, similar with properties, is influenced by the type of feedstock, production temperature, and production duration.

At the same production temperature of 300°C, the biochar produced from corn straw, penut straw, and soybean straw were all alkaline, but the pH of biochar from canola straw, wheat straw, and hull straw was 6.48, 6.42 and 6.43, respectively [22]. The biochar made at 350°C by [18] also demonstrated low pH at 5.38 in water.

The different biochar pH values between biochar and soil may be the main reason for soil pH change. Acidic biochar could also increase soil pH when used in soil with lower pH value. When biochar with a pH value of 5.38 was added into soil with a pH value of 4.33 and incubated at 30°C for 4 months, the soil pH value increased [16].

2.10 Chemical and physical Characteristics of Biochar

The char yield as well as, the chemical and physical characteristics of biochar depends on the nature of the feedstock's used (woody vs. herbaceous) and operating conditions and environment of the pyrolysis unit (low vs. high temperature, residence time; slow vs. fast pyrolysis, heating rate and feedstock preparation). The wide range of process parameters leads to the formation of biochar products that vary considerably in their elemental and ash composition, density, porosity, pore size distribution, surface area, surface chemical properties, water and ion adsorption and release, pH and uniformity of biochars' physical structure [28][23]. [26] Has proposed a classification scheme based on these characteristics to describe the differences in the quality of biochar. I refer the reader to that review for specific details.

The biochar yield from the pyrolysis of biomass is influenced by the pyrolysis temperature, its lignin, cellulose, and hemicellulose content and to a lesser extent the extractive concentrations of the feedstock [27][29]. Woody biomass with high lignin contents typically produce greater char yields than those derived from herbaceous feedstocks. A common feature among the various

pyrolysis processes is that C content of the biochar product shows a consistent increase with increasing temperature [30][31]. Biochars with large amounts of poly-condensed aromatic structures are obtained by pyrolyzing feedstocks at temperatures between 400 and 600°C [32][33]. Temperatures above 500°C commonly produce chars with C contents greater than 80 percent, at temperatures between 400 and 500°C biochars have C contents that range from 60 to 80 percent and biochars produced at low temperatures (< 350°C) have C content that varies from 15 to 60 percent[34].

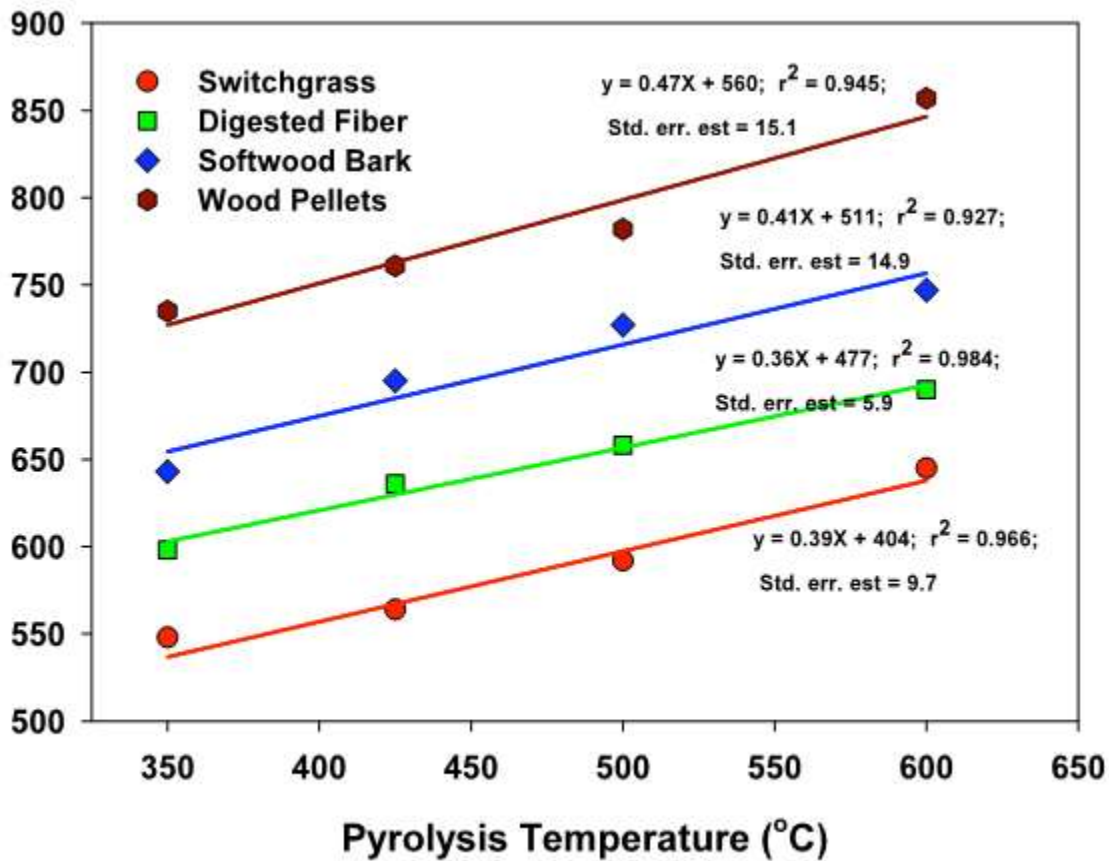


Figure 2: Relationship between pyrolysis temperature and the C concentration of the resulting biochar [35].

2.12 Impact of Biochar Applications on Soil Quality and Crop Productivity

Returning C to the soil in the form of biochar is an essential part of the integrated bioenergy-food production vision (Figure 3). Biochar applications to soils have been shown to enhance soil and

water quality. Because of its high surface area and high surface charge density [36], biochar increases the ability of soils to retain nutrients and plant available water and reduces leaching of nutrients and agricultural chemicals [37][29].

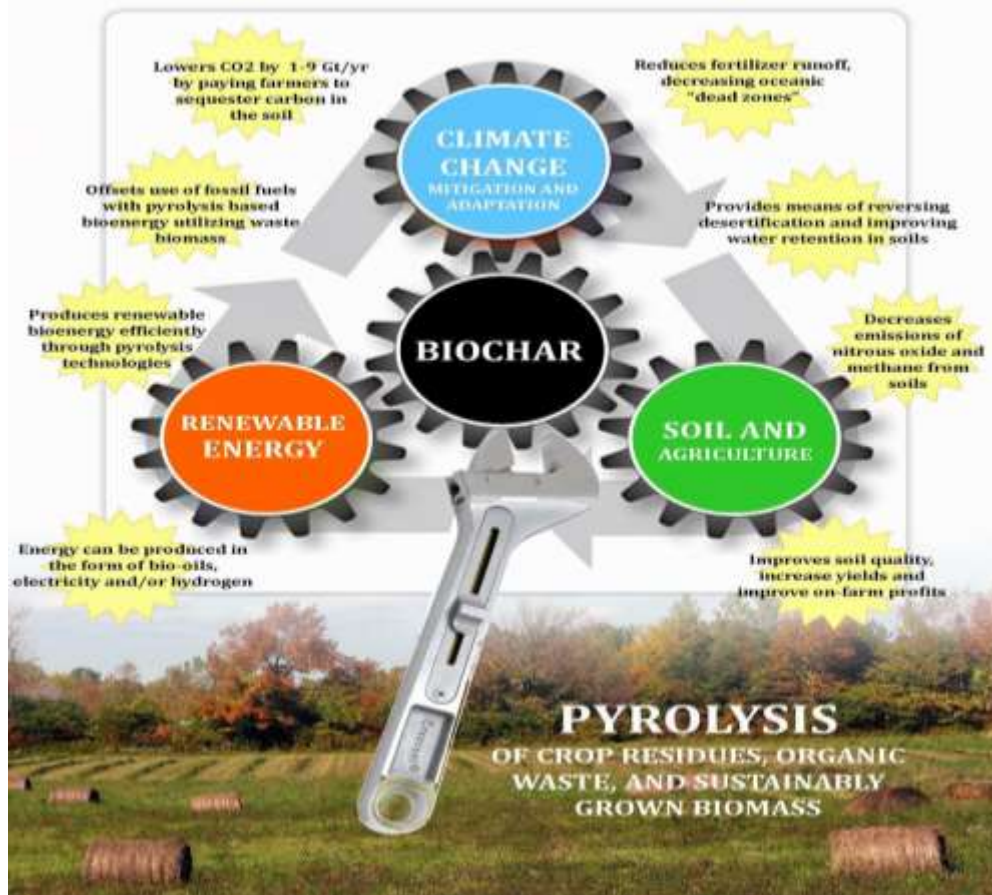


Figure 3: Schematic of biochar solution [38]

Soil biochar applications recycle most of the nutrients that are removed when biomass is harvested. Base cations (primarily Ca, Mg, and K) in biomass are transformed during pyrolysis into oxides, hydroxides, and carbonates (ash) that are mixed with the biochar.

Due to the presence of these bases most biochars function as a liming agent when applied to soil. Biochar is a low density material that reduces soil bulk density [39] and thereby increases water infiltration, root penetration, and soil aeration.

The improvements in crop productivity were related to increased nutrient retention [40][41]; alleviation of Al toxicity in highly acidic soils due to presence of Ca and Mg oxides, hydroxides and carbonates (ash) mixed with the biochar [40]; increased soil water permeability and plant water availability due to porous structure of biochar [42]; increased soil cation exchange capacity [43]; enhanced cycling of P and S [22]; and neutralization of phytotoxic compounds in the soil [44]. Moreover, biochar may indirectly influence plant growth by modify soil microbial communities. The above described-biochar induced increases in crop production occurred on highly weathered tropical soils where soil quality and nutrient availability are often limiting factors for crop productivity.

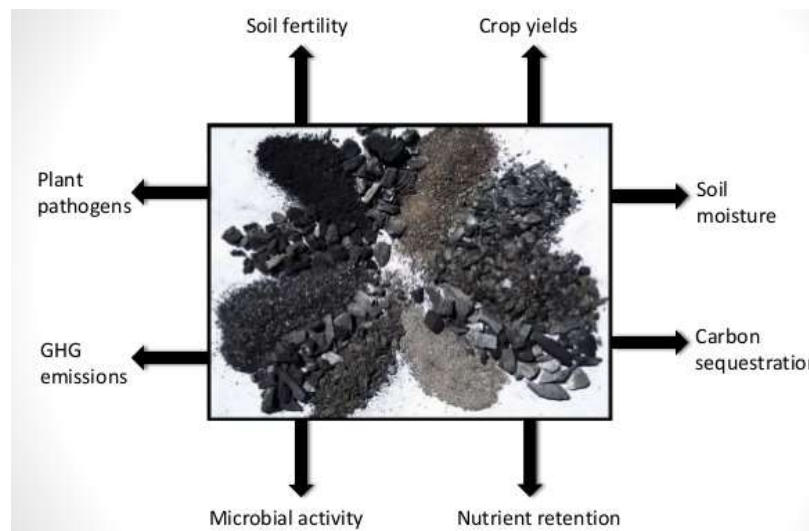


Figure 4: Functions of biochar

For highly productive temperate region soils, by contrast, weather is commonly the most important factor limiting crop yields rather than soil quality.

2.13 Using Biochar for carbon Sequestration in soil

It is generally accepted that reducing atmospheric concentrations of CO₂ by permanently sequestering C in the soil could reduce the impact of climate-related damage. Increasing soil organic carbon (SOC) storage by conventional soil management practices such as conservation tillage, no-till, and perennial cropping systems can take many years and there is uncertainty

about the C sequestration potential of these systems [24]. By contrast, application of biochar to agricultural soils is an immediate and easily quantifiable means of sequestering C and is rapidly emerging as a new management option that may merit high value C credits [40][45]. Soils low in organic matter typically exhibit the greatest increase in C with the addition of any biochar

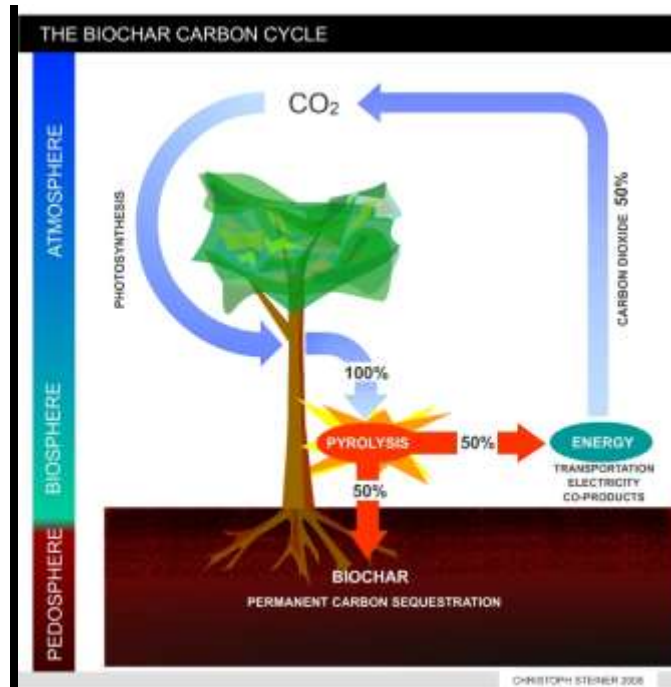


Figure 5: The biochar Carbon cycle

Biochar is highly stable in soil environments and tends to accumulate in the stable soil organic matter fraction [41]. Radiocarbon dating of charcoal has indicated mean residence times up to 10,000 years in soils [46][47]. Other studies have reported much shorter biochar half-lives ranging from <30 to several 100s of years [20][44].

The stability of biochar in soil environments depends on both the nature of the parent biological material and the extent of thermochemical alteration during pyrolysis. “Black-chars” produced by high temperature pyrolysis are believed to be biologically non-degradable and may persist in soils for millennia; whereas “brown-chars” produced at lower temperatures are biodegradable and persist in soils for shorter periods of time.

However, abiotic decomposition of biochar through chemical oxidation, photo oxidation, and solubilization also occurs, and C loss due to abiotic degradation may be 50 to 90 percent of that reported for biological degradation depending on charring temperature and volatile matter content of biochars [48].

Uncertainty associated with degradation rates of different biochars and an apparent potential for some biochars to accelerate decomposition of biogenic soil organic matter complicates assessment of biochar as a carbon sequestration agent. During a 500-day soil-column incubation study, biochar consistently increased CO₂ emissions relative to unamended controls, with cumulative CO₂-C loss equivalent to 18-23 percent of biochar C applied [49]. Production of biomass crops for the sole purpose of producing biochar as a means to withdrawing CO₂ from the atmosphere might be technically feasible, but is not likely to be economically viable in the foreseeable future.

The net effect of biochar on GHG emissions depends not only on the impact of biochar on the soil to which it is applied, but also on the macroeconomic impact of a pyrolysis-biochar industry on markets for food, feed, and any associate indirect land-use changes. Depending on those factors, the net values of GHG emissions can be negative (more CO₂ eq. reductions than emissions) or positive [50].

Adoption of new technology is often hindered by high startup costs, the need for market development, and unknown levels of risk associated with production costs. At this time, the greatest barriers to the viability of biochar as carbon sequestration tool are the high initial costs of designing, building and operating first generation biomass pyrolyzers with heat recovery and the lack of viable markets for biochar. The development of higher value engineered biochars able to play agronomical functions in targeted soils could also contribute to improve the economic viability of this technology.

The value of carbon credits is currently too low to provide an incentive for farmers to apply biochar to their land and fossil fuels are still relatively inexpensive. In the future, however, dwindling global supplies of petroleum and concerns over global climate change may prompt

changes in Federal policy that increase the value of both renewable energy and carbon credits and prompt wider use of biochar as soil amendment [41]

2.14 Recommendation by Past Researchers

The research that has been undertaken for this thesis has highlighted topics on which further research would be beneficial. In packaging this biochar based fertilizer development, design and testing of compost Pelleting machine and evaluating the fertilizer using the existing fertilizer application technologies will be essential.[51]. Coupling of the Pyrolysis system with the combustion simulation for these stove designs, in consideration of volatile gas in increasing the heat transfer within the bed[25].

The use of single (metal) container to two barrels is common, while some units are built of ceramic materials like fired brick[52]. Before wide-spread implementation of biochar-producing cook stoves, significant research efforts must be made to quantify energy output, biochar quantity and quality with different feedstocks available to smallholder farmers and comparing different cook stove designs. In addition, research is needed assessing the emissions associated with different designs of pyrolytic cook stoves[53]

2.15 Research gaps still to be addressed

The heat transferred from the inner to outer stove is not enough to produce more qualified biochar for one round of cooking because of large diameter of outer cylinder and the supplied heat is only from the inner combustion chamber of the stove [54].

The produced biochar pH at the inners side is not equal with the outer side of the stove because of the high temperature variation [55].

The efficiency of pyrolytic stoves are still less and it needs the design optimization of the combustion chamber. The weight of the stove with biomass to be charred is also another issue that should be addressed [53]. However, CFD modeling for biomass still face significant challenge for pyrolysis due to the complexity of the biomass feedstock and the thermochemical process [23]

Biomass is a mixture of hemicellulose, cellulose, lignin and minor amounts of other organics with proportion and chemical structure affected by variety. Inorganic ash is also part of the biomass composition [23].

2.16 Scope of the research

The scope of work is mentioned by the following points:

- i. Desk study and literature review of the stove design parameters, characterizations of different type of scenarios materials and technologies being adopted in Ethiopia and in different parts of the world.
- ii. Develop the CFD simulation, design modification, characterization, and to address the Knowledge gaps.
- iii. Prepare detailed specifications of all the required parameters (including, Area of the combustion chamber, heat transfer, power output materials, dimensions, application, biomass type etc.)
- iv. Fabricate the stove and do the experimental validation of cook stove design testing to establish performance of the stove and come up with practical solutions
- v. Conduct field testing in the suitable socio-economic and geo-physical conditions where the ultimate dissemination of developed stove would be desired/ recommended.

CHAPTER THREE

3. RESEARCH METHODOLOGY AND DESIGN BASIS

3.1 Description of the Study Area:

The study was conducted in Jimma University, Southwest Ethiopia in the year 2016. It is located at 7°, 33 N and 36°, 57' E at an altitude of 1710 meter above sea level. The mean annual maximum and minimum temperatures are 26.8°C and 11.4°C and humidities are 91.4% and 39.92%, respectively. The mean annual rainfall of the study area is 1500mm [24][4].

3.2 Materials

3.2.1 Materials used for the fabrication and experimental Test

Sheet metals	Fuel (wood)
Tongs for handling charcoal	Digital thermometer
Metal tray to hold charcoal	Infrared thermometer
Biomass (coffee husk, sawdust)	Digital multi-meter
Wood moisture meter	Thermocouple
Elemental analysis equipment	Cooking pot
Surface area and bulk density analysis equipment	Mass balance
Weighing	Shaking machine
pH meter	Beakers
Scale	Electrode
Grinder	Chemicals
Timer	Moisture meter
Water	Watch

3.3 Methods used

To improve the above problems Designing modification, CFD simulation and experimental validation of the proposed cooking stoves undergo several methodologies.

3.2.2 Computational fluid dynamics analysis

3.2.2.1 Overview

The Analytical design and sizing, heat transfer, combustion are the first steps to be done to fix size and geometry of cooking stove. After the designing of geometry and size of the stove is finished the CFD modeling and simulation involves several simulation and iteration for different scenarios to analyze Combustion efficiency, heat transfer, turbulent combustion, analysis.

The three-dimensional continuous feeding biochar producing stove model is based on the geometry and operational conditions of the primary and secondary chambers. The following components of the model will be described in detail:

3.2.2.2 Geometry

The model is done by ANSYS 14.5 software. As shown in Figure 7, the main portion of the flow domain is a cylindrical chamber with a gradual flow contraction near the top. 120 small diameters of circular holes air inlets are distributed at the bottom of the chamber after different models were taken. There are no air inlets on the side of the chamber to allow proper flow of flame from bottom part of the stove to top and to reduce the turbulence of flame. A rectangular port on the side of the chamber allows for fuel to be rammed into the chamber. A vertical outlet cylinder extends from the top of the chamber. In reality, this outlet is short and connects to a removable cone chamber where secondary air is added; this cone chamber is connected in turn to the outer cylinder of chamber.

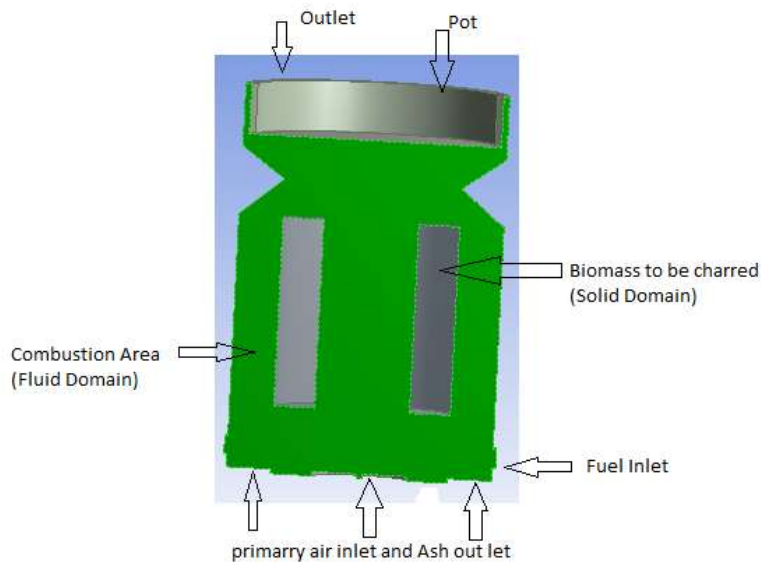


Figure 6 : 3D geometry of the stove

3.2.2.3 Computational Mesh and Boundary conditions

The domain geometry and the computational mesh were generated using the ANSYS 14.5 software package. The mesh is a structured, hexahedral mesh, except for a small region around the grate in which an unstructured, tetrahedral mesh was used. The use of a structured, hexahedral mesh is beneficial, allowing for decreased computational time to achieve converged solutions. The grid used for the majority of model runs contained 182,675 elements. This is a relatively coarse grid; however, the complexity of the problem dictated that even so, fully converged solutions required on the order of 48 hours to achieve. A finer grid would increase this solution time even further. It was determined that fine resolution of the temperature, velocity, and turbulence fields was not required to achieve a suitable overall solution.



Figure 7: Mesh geometry

3.2.2.4 Fluid dynamics and turbulence models


Fluid flow within the 3D chamber was modeled under incompressible, steady state conditions. A segregated, cell-based, implicit solver was used to achieve the solution. The standard k-epsilon turbulence model with a standard wall function was employed.

The inputs for the model include

- Fuel composition
- Fuel supply rate
- Initial temperature of fuel and air

The following flow boundary conditions were imposed:

- **Inlets:** Two separate mass flow inlet zones were defined. 120 small holes of primary air inlets at the bottom of the chamber comprise the first zone, while the side fuel port was defined as a secondary air inlet

 Mass Flow Rate	(kg/s)
Air_inlet_1	= 0.0055000024
Air_inlet_2	= 0.0055000292
Fuel_inlet	= 9.1582857e-05

- **Outlet:** The exit of the outlet pipe was defined as an outlet
- **Walls:** All other surfaces within the domain were defined as walls, with a no-slip condition and a roughness coefficient of 0.5.

3.2.2.5 Heat transfer and the governing Equations of Natural Convection

When heat is added to a gas, specifically air in the case of a stove, it expands, and thus changes density. The presence of gravity and change of density induces a change in the body forces, and the forces cause the fluid to move "by itself" without any externally imposed flow velocity. This is the phenomenon of natural convection. This phenomenon would occur throughout the stove, and the main driving force for the fluids flow would be buoyancy, inflicted by high a temperature gradient.

The governing equations for natural convection flow are of a considerable complexity. The governing equations of Natural Convection are therefore defined by (equation set 3.1 to 3.4)

Mass balance equation

$$\frac{\partial u}{\partial x} + \frac{\partial v}{\partial y} = 0 \quad (3.1)$$

Energy equation

$$u \frac{\partial T}{\partial x} + v \frac{\partial T}{\partial y} = \alpha \frac{\partial^2 T}{\partial y^2} \quad (3.2)$$

Momentum equation

$$u \frac{\partial u}{\partial x} + v \frac{\partial u}{\partial y} = \beta g (T - T_{\infty}) + \nu \frac{\partial^2 u}{\partial y^2} \quad (3.3)$$

Where the coefficient of volumetric thermal expansion,

$$\beta = -\frac{1}{\rho} \left(\frac{\partial \rho}{\partial T} \right)_p = \frac{1}{\rho} \left(\frac{p}{RT^2} \right) = \frac{1}{T} \quad (3.4)$$

Energy transport and radiation equations were enabled to account for heat transfer throughout the chamber via conduction, convection, and radiation. The P1 radiation model was used. The specific heat of each component gas was represented by a piecewise polynomial function.

The following energy boundary conditions were applied:

- **Inlets:** An inlet temperature of 320 K was set for both air inlets.
- **Walls:** An insulated (heat flux = 0) boundary condition was set on all walls.

3.2.1.6 Species transport and reaction model

The full “species transport” model was employed to simulate the transport and reaction of chemical species within the combustor. Volumetric reactions were enabled, and the eddy dissipation model was used to represent the interaction between turbulence and chemical reactions.

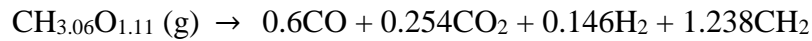
When you choose to solve conservation equations for chemical species, ANSYS Fluent predicts the local mass fraction of each species, through the solution of a convection-diffusion equation for the species. This conservation equation takes the following general form:

$$\frac{\partial}{\partial t}(\rho Y_i) + \Delta \cdot (\rho \bar{v} Y_i) = -\nabla \cdot \bar{J}_i + R_i + S_i \quad (3.5)$$

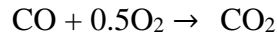
Where R_i the net is rate of production of species i by chemical reaction and S_i is the rate of creation by addition from the dispersed phase plus any user-defined sources. An equation of this form will be solved for $N-1$ species where N is the total number of fluid phase.

Thus, neither reaction kinetics nor equilibrium chemistry was used to determine the chemical reactions; reaction rates were dependent strictly on turbulent mixing. Five chemical reactions were defined as follows:

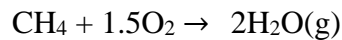
3.2.1.7 Decomposition of volatiles



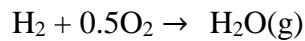
Combustion of volatiles:



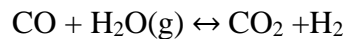
Combustion of Methane:



Combustion of H₂



Water-gas shift reactions



The volatiles “molecule”, CH_{3.06}O_{1.11}, is meant to symbolize the variety of volatile compounds released via pyrolysis. The chemical subscripts for H and O elements within this molecule represent the ratio of H:C and O:C respectively, after subtracting the fraction of C that goes to fixed carbon (char).

3.2.2 Construction

After the different CFD simulation of the stove and optimum results are obtained the fabrication of the cook stove is followed. A thick steel grate is located near the bottom of the chamber to support the biomass fuel bed



Figure 8: Constructing the continuous feeding biochar producing stove

3.2.3 Experimental validation

Once the fabrication is completed the experimental validation is continued.

3.2.3.1 Selection of fuels for testing

The fuels that are used in this cook stove are selected first by collecting different types of fuels from the different areas of the villages. I have collected different agricultural residues locally from the village in Jimma town and Gera district nearby Jimma city. Biomass species were collected including coffee husk and sawdust, and dried in an oven at 105°C to remove fuel moisture content. In present study, biomass fuel has been selected on the basis of proximate and ultimate analysis.

3.2.3.2 Description of selected pyrolysis stoves

Since the biomass selected to be char is coffee husk and sawdust the indirect pyrolytic stoves (normal Anila and continuous feeding Anila type stoves) are selected to compare the performance of the new stove.

3.2.3.2.1 Anila stove

Anila-type stoves use two concentric cylinders of different diameters (see Figure 10). Biomass fuel is placed between the two cylinders and a fire is ignited in the center. Heat from the central fire pyrolyzes the concentric ring of fuel. The gasses escape to the center where they add to the cooking flame as the ring of biomass turns to char.

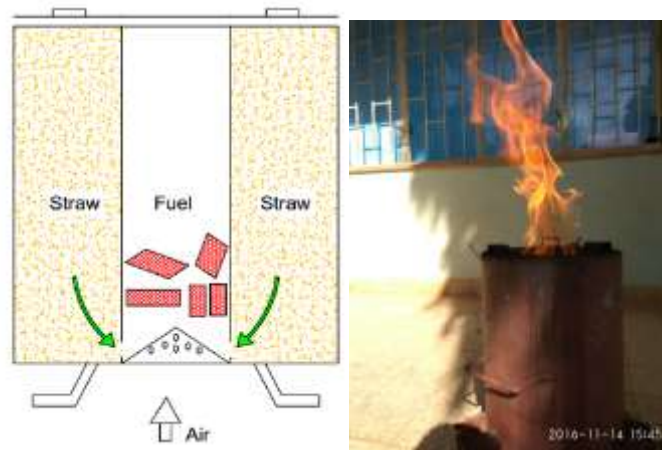


Figure 9: Normal Anila stove

3.2.3.2.2 Continuous feeding Anila type stove

Continuous feeding anila type stove was done by Mr. teka tesfaye at Jimma university and modified to make the burning fuel (wood) Continuous, Reduced height and increased outer diameter with flange tightened at six place using bolt and nut.



Figure 10: continuous feeding anila type stove

3.2.3.3 Continuous feeding biochar producing cook stove-firing practice

This was studied by observation of actual cooking, a questionnaire survey, and measurement of biochar formation and temperature at different parts of hearth zone, and direct experience of

cookstove firing . The followings are the observations:

- (1) Kerosene is used for the initial ignition of firewood. Comparatively dried and smaller diameter wood is preferred for the initial burning. It usually takes 2 to 3 min to achieve a steady-state flame.
- (2) Usually, two or three larger diameter wooden sticks (4 to 6 cm) and a few smaller diameter Sticks (2 to 4 cm) are fired simultaneously to attain the required heating rate.
- (3) In general, 50 to 70 cm long wood sticks are preferred so that the fire can be adjusted easily by slight movement of these sticks. Firewood is arranged in such a manner that sufficient primary air can pass through the fuel feed port.
- (4) If necessary, we can blow air by mouth to maintain a good flame size.
- (5) Red hot charcoal helps sustain the flame. It is necessary to remove the excess charcoal if it is accumulated in the hearth zone to make space for the firewood.
- (6) The woman who is cooking sits on one side of the cook stove to avoid exposure to radiated heat from the wood insertion hole.

3.2.3.3 Calculation of WBT performance metrics

The Water Boiling Test (WBT) is a simplified simulation of the cooking process. It is intended to measure how efficiently a stove uses fuel to heat water in a cooking pot and the quantity of emissions produced while cooking. The WBT test for efficiency can be performed throughout the world with simple equipment. (If emissions are measured, more complex equipment is required.) Its primary benefits are:

- Provide initial or laboratory assessments of stove performance in a controlled setting
- Compare the effectiveness of different designs at performing similar tasks
- Evaluate stove changes during development
- Select the most promising products for field trials
- Ensure that manufactured stoves meet intended performance based on designs



Figure 11: Sample of water boiling test and measuring temperature for the selected stoves

The WBT consists of three phases: a high-power phase with a cold start, a high power phase with a hot start, and a low power (simmering) phase. Each phase involves a series of measurements and calculations. The calculations for the one-pot test are described below

Variables that are constant throughout all three phases

HHV	Gross calorific value (dry wood) (kJ/kg)
LHV	Net calorific value (dry wood) (kJ/kg)
MC	Wood moisture content (% - wet basis)
EHV	Effective calorific value (accounting for moisture content of wood)
LHV_{char}	Net calorific value of char (kJ/kg)
P_1	Dry mass of empty pot (grams)
K	Weight of empty container for char (grams)
T_a	Ambient Temperature ($^{\circ}C$)
T_b	Local boiling point of water ($^{\circ}C$)

3.2.3.3.1 Determination of Moisture Content:

The moisture content of fuel is necessary to be determined to calculate the efficiency of the stove. The standard test methods for determination of moisture content using a microwave oven by American Society for Testing and Materials Committee E48.05 on biomass conversion was used [56]. Moisture content of the samples was calculated as the percentage difference between the wet weight and the dry weight using equations 1 and 2 proposed by Maker [57].

$$MC = \frac{m_{\text{fuel,wet}} - m_{\text{fuel,dry}}}{m_{\text{fuel,wet}}} \quad (3.6)$$

MC is a decimal fraction which is formatted in the WBT spreadsheet as a percentage. Therefore, if the spreadsheet shows that MC = 15%, a value of MC =0.15 is used for the calculations.

3.2.3.3.2 Computation of Gross Calorific Value:

The Gross Calorific Values/Higher Heating Values from the bomb calorimeter results were calculated using equation below.

$$HHV = \frac{\Delta T \times M_T}{W_s} \times SPH_w \quad (3.7)$$

Where, T is temperature rise, M_T is total water equivalent, W_s is weight of sample, SPH_w is specific heat capacity of water. Similarly, the higher calorific values were calculated from proximate and ultimate analysis using equation 5.

$$HHV = 0.3491C + 1783H - 0.1034O - 0.0211A + 0.1005S - 0.0151N \quad (3.8)$$

Where, HHV is higher heating value/Gross calorific value, C is weight fraction of carbon; (wt %), H is weight fraction of hydrogen; (wt %), O is weight fraction of oxygen; (wt %), A is weight fraction of ash; (wt %), S is weight fraction of sulphur (wt %) and N is weight fraction of nitrogen appearing in the ultimate analysis (wt %). This formula was selected because it gives an average error of 1.45 %, typical of the error of most measurements. This equation permits using heat values in calculations and models of biomass processes [6].

3.2.3.3.3 Computation of Lower Heating Values:

Lower heating value (LHV) or net calorific value (NCV) from the proximate and ultimate analysis results was computed using equation below [21].

$$LHV = HHV \left(1 - \frac{m_{wb}}{100} \right) - 2.447 \times \frac{m_{wb}}{100} - \frac{H}{200} \times 18.02 \times 2.447 \left(1 - \frac{H}{100} \right) \quad (3.9)$$

Where, LHV is lower heating value in kJ/kg, HHV is higher heating value in kJ/kg, Mwb is moisture content measured wt % and H is hydrogen content wt % .

3.2.3.3.4 High power phase (cold start)

The stove is initially at a cold state and a fire is lit/kindled in this state until a steady flame is reached. Upon reaching a steady flame, a timer is started and the boil test timing begins.

3.2.3.3.4.1 Variables that are measured directly

- f_{ci} Mass of fuel before test (grams)
- P_{1ci} Mass of pot of water before test (grams)
- T_{1ci} Water temperature at start of test (°C)
- t_{ci} Time at start of test (min)
- f_{cf} Mass of fuel after test (grams)
- c_c Mass char with dish after test (grams)
- P_{1cf} Mass of pot of water after test (grams)
- T_{1cf} Water temperature at end of test (°C)
- $t_{cf} =$ Time at end of test (min)

3.2.3.3.4.2 Variables that are calculated

f_{cm}	Fuel consumed, moist (grams)
Δc_c	Change in char during test (grams)
f_{cd}	Equivalent dry wood consumed (grams) Water vaporized (grams)
w_{cv}	Effective mass of water boiled (grams)
Δt_c	Time to boil (min)
Δt_c^T	Temperature corrected time to boil (min)
h_c	Thermal efficiency (%)
r_{cb}	Burning rate (grams/min)
SC_c	Specific fuel consumption (grams wood/liter water)
SC_c^T	Temp-corrected specific fuel consumption (grams wood/grams water)
SE_c^T	Temp-corrected specific energy consumption (kJ/liter water)
FP_c	Firepower (W)

Fuel consumed: Is the mass of wood used to bring the water to a boil, found by taking the difference of the pre-weighed bundle of wood and the wood remaining at the end of the test phase:

$$f_{cm} = f_{ci} - f_{cf} \quad (3.10)$$

Where f_{cm} = fuel consumed, moist

f_{ci} = mass of fuel before test

f_{cf} = mass of fuel after tes

Net change in char: The net change in char during the test is the mass of char created during the test, found by removing the char from the stove at the end of the test phase. Because it is very hot, the char will be placed in an empty pre-weighed container of mass k (to be supplied by testers) and weighing the char with the container, then subtracting the container mass from the total:

$$\Delta c_c = c_c - k \quad (3.11)$$

Where, Δc_c = Change in char during test

c_c = Mass of char with container after test (g)

k = Mass of container (g)

Mass of water vaporized: The mass of water vaporized is a measure of the water lost through evaporation during the test. It is calculated by subtracting the initial weight of pot and water minus final weight of pot and water shown in equation below.

$$w_{cv} = p_{1ci} - p_{1cf} \quad (3.12)$$

Where, w_{cv} = Water vaporized (g)

p_{1ci} = Mass of pot of water before test (g)

p_{1cf} = Mass of pot of water after test (g)

Effective mass of water boiled: The effective mass of water boiled is the water remaining at end of the test. It is a measure of the amount of water heated to boiling. It is calculated by simple subtraction of final weight of pot and water minus the weight of the pot shown in equation below.

$$w_{cr} = p_{1cf} - p_1 \quad (3.13)$$

Where, w_{cr} = Effective mass of water boiled (g)

p_{1cf} = Mass of pot of water after test (g)

p_1 = Mass of pot (g)

Time to boil: The time to boil is the difference between the time when the water starts to boil and the initial time when the pot was placed on the stove. The equation for time to boil is shown in equation below.

$$\Delta t_c = t_{cf} - t_{ci} \quad (3.14)$$

Where Δt_c = Time to boil (min)

t_{cf} = Time at end of test (min)

t_{ci} = Time at the start of test (min)

Temperature-corrected time to boil: The temperature-corrected time to boil pot #1 is the same as above, but adjusts the result to a standard 75 °C temperature change (from 25 °C to 100 °C). This adjustment standardizes the results and facilitates a comparison between tests that may have used water with higher or lower initial temperatures.

$$\Delta t_c^T = \Delta t_c \times \frac{75}{T_{1cf} - T_{1ci}} \quad (3.15)$$

Where, Δt_c^T = Temperature-correlated time to boil (min)

Δt_c = Time to boil (min)

T_{1cf} = Water temperature at end of test (°C)

$$T_{1ci} = \text{Water temperature at start of test } (^{\circ}\text{C})$$

Equivalent dry fuel consumed: The equivalent dry fuel consumed adjusts the amount of dry fuel that was burned in order to account for two factors: (1) the energy that was needed to remove the moisture in the fuel and (2) the amount of char remaining unburned. The mass of dry fuel consumed is the moist fuel consumed minus the mass of water in the fuel. The equation for the mass of dry fuel is shown in equation below

$$Dry_{fuel} = f_{cm}(1 - MC) \quad (3.16)$$

$$f_{cd} = \frac{f_{cm} [LHV(1 - MC) - MC [4.186(T_b - T_a) + 2257]] - \Delta c_c (LHV_{char})}{LHV} \quad (3.17)$$

Where, Dry_{fuel} = Amount of dry fuel (g)

$$f_{cm} = \text{Fuel consumed, moist (g)}$$

$$MC = \text{Moisture content}$$

$$LHV = \text{Low heating value (net caloric value (KJ/Kg))}$$

$$LHV_{char} = \text{Char calorific value (KJ/1Kg)}$$

Thermal efficiency: The efficiency of a stove is usually defined as the ratio of heat utilized by the pot to cook food to the heat produced by fuel. Thermal efficiency is the significant parameter to find out performance of the stove. Heat transfer efficiency of stove is defined as the ratio of heat utilized by the pot to the heat produced by the fuel. The equation for thermal efficiency is shown in equation below.

$$h_c = \frac{4.186(T_{1cf} - T_{1ci})(P_{1ci} - P_1) + 2260(w_{cv}) \times 100\%}{f_{cd}(LHV)} \quad (3.18)$$

Where, h_c = Thermal efficiency

T_{1ci} = Water temperature at start of test ($^{\circ}C$)

T_{1cf} = Water temperature at end of test ($^{\circ}C$)

P_{1ci} = Mass of pot water after test (g)

P_1 = Mass of pot (g)

LHV = Net calorific value

w_{cv} = Water vaporization (g)

f_{cd} = Equivalent dry fuel consumed (g)

Burning rate: This is a measure of the rate of fuel consumption while bringing water to a boil. It is calculated by dividing the equivalent dry fuel consumed by the time of the test.

$$r_{cb} = \frac{f_{cb}}{d_{tc}} \quad (3.19)$$

Where, r_{cb} = Burning rate (g/min)

f_{cb} = Equivalent dry fuel consumed (g)

d_{tc} = Time to boil (min)

Specific fuel consumption: Specific consumption can be defined for any number of cooking tasks and should be considered “the fuel required to produce a unit output” whether the output is boiled water, cooked beans, or loaves of bread. In the case of the cold-start high-power WBT, it is a measure of the amount of wood required to produce one liter (or kilo) of boiling water starting with cold stove. It is calculated as:

$$s_{cc} = \frac{f_{cd}}{w_{cv}} \quad (3.20)$$

Where, s_{cc} = Specified fuel consumption (g fuel/L of water)

f_{cd} = Equivalent dry fuel consumed (g)

w_{cv} = Effective mass of water boiled (g)

Temperature corrected specific fuel consumption: The temperature corrected fuel consumption is the factor used to correct the fuel consumption which normalizes the initial water temperature difference of stoves being tested in a different day or different condition to standard change in temperature of 75°C (25°C to 100°C).

The equation for temperature corrected specific fuel consumption is shown in equation below.

$$sc_c^T = sc_c \times \frac{75}{T_{1ef} - T_{1ci}} \quad (3.21)$$

Where, sc_c^T = Temperature corrected specific fuel consumption (g fuel/g water)

sc_c = Specific fuel consumption (g)

T_{1ci} = Water temperature at start of test (°C)

T_{1ef} = Water temperature at end of test (°C)

Temperature corrected specific energy consumption: Similar to the temperature corrected specific fuel consumption, this metric is a measure of the amount of fuel energy required to produce one liter (or kilo) of boiling water starting with cold stove. It is the temperature corrected specific fuel consumption multiplied by the energy content of the fuel:

$$SE_c^T = SC_c^T \times \frac{LHV}{1000} \quad (3.22)$$

Fire power: The fire power is defined as the amount of energy of the fuel used to bring the water to a boil divided by duration to boil the water. The equation for fire power is shown in equation below.

$$FP_c = f_{cd} \times LHV \quad (3.23)$$

$$FP_c = \frac{f_{cd} \times LHV}{\Delta t_c \times 60} \quad (3.24)$$

Where, FP_c = Fire power

f_{cd} =Equivalent specific fuel consumption

LHV = Net caloric value

Δt_c = Time to boil (min)

Turn-down ratio: The turn down ratio of the average high fire power to the average low fire power.it serves as a representation of the degree in which the user can adjust the fire power of the stove. The equation for the turn-down ratio is shown in equation below.

$$TDR = \frac{FP_c}{FP_s} \quad (3.25)$$

Where, TDR = Turn-down ratio

FP_c = Fire power during cold start (W)

FP_s = Fire power during simmering (W)

3.2.3.3.4.3 High power test (hot start)

This test must follow directly after another burn test (usually a cold start test). This is simply due to the fact that this test revolves around starting a new fire after the stove is heated up from previous use (to simulate sequential cooking of meals/dishes). This new fire is set up in a clean chamber (ash is cleaned out and weighed for the previous test). The test setup is exactly the same

as the aforementioned cold start test, but the only difference is substitute the subscript “c” instead of “h” for each variables.

Variables that are directly measured

- f_{hi} = Mass of fuel before test (grams)
- P_{1hi} = Mass of pot of water before test (grams)
- T_{1hi} = Water temperature at start of test (°C)
- t_{hi} = Time at start of test (min)
- f_{hf} = Mass of fuel after test (grams)
- c_h = Mass char with dish after test (grams)
- P_{1hf} = Mass of pot of water after test (grams)
- T_{1hf} = Water temperature at end of test (°C)
- t_{hf} = Time at end of test (min)

3.2.3.3.4.4 Low power test (simmering)

The simmer reached in test two is to be maintained for 45 minutes and the amount of added fuel during this time period is measured. This measured amount of fuel will still be added to the total amount of fuel used (as both test types are conducted in one test).

Variables that are directly measured

- f_{si} = Starting mass of fuel (grams)
- P_{1si} = Starting mass of pot with water (grams)

T_{1si} = Starting water temperature (°C)

$t_{s,i}$ = Time at start of simmer phase (min)

f_{sf} = Mass of unburned fuel remaining after test (grams)

c_s = Mass of charcoal and container after test (grams)

P_{1sf} = Mass of pot with water after test (grams)

T_{1sf} = Water temperature at end of test (°C)

t_{sf} = Time at end of simmer phase (min)

Fuel consumed, moist (grams)

$$f_{sm} = f_{si} - f_{sf} \quad (3.26)$$

Change in char during test (grams)

$$\Delta c_s = c_s - k \quad (3.27)$$

Water vaporized (grams)

$$w_{sv} = p_{1si} - p_{1sf} \quad (3.28)$$

The effective mass of water simmered (grams)

$$w_{sr} = p_{1sf} - p_1 \quad (3.29)$$

Time to boil (min)

$$\Delta t_s = t_{sf} t_{si} \quad (3.30)$$

Equivalent dry fuel consumed (grams)

$$f_{sd} = \frac{f_{sm}(LVH(1-mc) - mc(4.186(T_b - T_a) + 2257)) - \Delta c_s \times LVH_{char}}{LVH} \quad (3.31)$$

Thermal efficiency %

$$h_s = \frac{4.186 \times (T_{1sf} - T_{1si}) \times (p_{1si} - p_1) + 2660 \times w_{sv}}{f_{sd} \times LHV} \quad (3.32)$$

Burning rate (grams/min)

$$r_{sb} = \frac{f_{sd}}{\Delta t_s} \quad (3.33)$$

Specific fuel consumption (grams wood/liter water)

$$SC = \frac{f_{sd}}{w_{sr}} \quad (3.34)$$

Specific energy consumption (KJ/liter water)

$$SE_s = SE_c \times \frac{LHV}{1000} \quad (3.35)$$

Firepower (W)

$$FP_s = \frac{f_{sd} \times LHV}{\Delta t_s \times 60} \quad (3.36)$$

Torn down ratio

$$TDR = \frac{FP_c}{FP_s} \quad (3.37)$$

3.2.3.4 Biochar laboratory test

After the simulation and fabrication of the stove is completed once, the WBT test is taken to analyses the performance of constructed stove and to test the biochar physical and chemical properties are determined. The biochar laboratory test was done at chemical engineering department and college of Agricultural and Veterinary medicine

3.2.3.4.1 Biochar Analysis

After the three stoves had cooled sufficiently to handle, the bottom flanges of Anila stove and continuous biochar producing stove and the top part of new stove were removed and the char produced were emptied into a plastic bags of known weight. The bags and their contents were weighed to the nearest gram using a weighing scales. The weight of the biochar were then calculated by subtracting the known weight of the bags.

Bagged samples were set aside until all experimental burns were complete to ensure that all chemical analyses took place simultaneously, as temperature proved to be a significant variable in pH and conductivity measurements.

3.2.3.4.2 Determination of Physical and chemical Parameters of produced biochar

i) Bulk density

The bulk density of material was determined as per the standard procedure. A cylindrically shaped container of 1000 ml volume was used for determination. The container was weighed empty to determine its mass and then it was filled with the sample and weighed once again. The bulk density was determined by dividing the mass of the material by the volume of the container [58]. The bulk density was calculated by using the formula:

$$\text{Bulk density (Kg/m}^3\text{)} = \frac{\text{Mass of biochar (Kg)}}{\text{Volume of measuring cylinder, (m}^3\text{)}} \quad (3.28)$$

ii) Bio char Yield

Conversion efficiency of biochar was calculated using the following equation: [55]

$$\text{Conversion efficiency (\%)} = \frac{\text{Weight of biochar}}{\text{Weight of feedstock used}} \times 100 \quad (3.29)$$

3.2.3.4.3 Determining Biochar specific surface area

Surface area per gm of the biochar was obtained using Sears method, Sears 1956 [45][25]. 1.5 gm of biochar sample was mixed with 100 ml of water and 30 gm NaCl. The mixture was stirred for five minutes. To this 0.1 N HCl was added to make final volume 150 ml and final pH = 4.0. It was then titrated against 0.1N NaOH. The volume (ml) of 0.1N NaOH required to raise the pH from 4.0 to 9.0 was noted. The specific area (i.e. area per gm) was obtained using the formula

$$A = 32V - 25 \quad (3.30)$$

Where, A = Surface area of carbon per gm (in m²/gm);

V = volume of 0.1N NaOH required to raise the pH from 4.0 to 9.0.

3.2.3.4.4 Biochar pH value

The pH of coffee husk and sawdust from different three stoves was determined by agitating the sample in deionized water (DW) at a solid/liquid ratio of 1/10 (g/mL) for a period of 1hour. The pH of the three produced biochars from coffee husk and was measured in DW and in KCl 1N with a solid/liquid (g/mL) ratio of 1/10[25].

The pH of Biochar solution is depend on the pyrolysis condition and the type of feedstock [12]. The pH of high Temperature case is greater than that of the low temperature heating case which is more alkaline [8]

3.2.3.4.3 Proximate analysis of biochar

The proximate analysis of the samples was carried out in the college of Agricultural and Veterinary medicine Laboratory at the Department of soil Science, and in the Jimma Institute of technology at the departments of chemical, while ultimate analysis was carried out at environmental engineering Laboratories, Jimmma University. The proximate analysis was used to determine the moisture content, volatile content, free carbon, and ash. The ultimate analysis was used to determine carbon, hydrogen, oxygen, nitrogen and sulphur

i) Determination of Volatile Matter (PVM)

The content of volatile matter was determined by heating the samples out of contact with air in a furnace to 950°C ±10°C for seven minutes [56]. The percentage mass of volatile matter was

calculated from the loss in mass of the sample after reducing the loss in mass due to moisture. The percentage of sample mass that remained after removal of volatile matter and ash content was determined to give the fixed carbon content. Each parameter was determined in triplicates.

$$PVM = \frac{A - B}{A} \times 100 \quad (3.31)$$

Where A is the weight of the oven dried sample and B is the weight of the sample after seven min in the furnace at 550°C.

ii) Ash Content

Ash content is the noncombustible residue left after fuel is burnt. It represents the bulk mineral matter after carbon, oxygen, sulphur and water have been driven off during combustion. The ash content was calculated from the residue that remained after samples were heated in a furnace [59].

The residual sample in the crucible was heated without lid in a muffle furnace at 700 ± 50 °C for one half hour (ASTM D- 3174). The crucible was then taken out, cooled first in air, then in desiccators and weighed. Heating, cooling and weighing was repeated, till a constant weight was obtained. The residue was reported as ash on percentage basis.

$$A.C(\%) = \frac{W_3 - W_1}{W_2 - W_1} \times 100 \quad (3.32)$$

Where, W_1 = weight of empty crucible, g

W_2 = weight of crucible + sample taken from stage (II),

W_3 = weight of crucible + ash left in crucible, g

iii) Fixed Carbon Content

The fixed carbon content was calculated by applying the mass balance for the biomass sample.

$$FC, (\%) = 100 - \%, \text{ of } (MC + VM + AC) \quad (3.33)$$

Where, FC = Fixed carbon, (%)

MC = Moisture content, (%)

VM = Volatile matter, (%), AC = Ash content, (%)

CHAPTER FOUR

4. RESULTS AND DISCUSSION

4.1 Simulation results

The CFD simulation of the stove was done by ANSYS 14.5 version. The flow of gas, heat transferred by conduction from combustion chamber to pot was simulated. The effect of element size, direction of air flow and temperature trend was discussed below.

4.1.1 Transient heat transferred through the stove and biochar

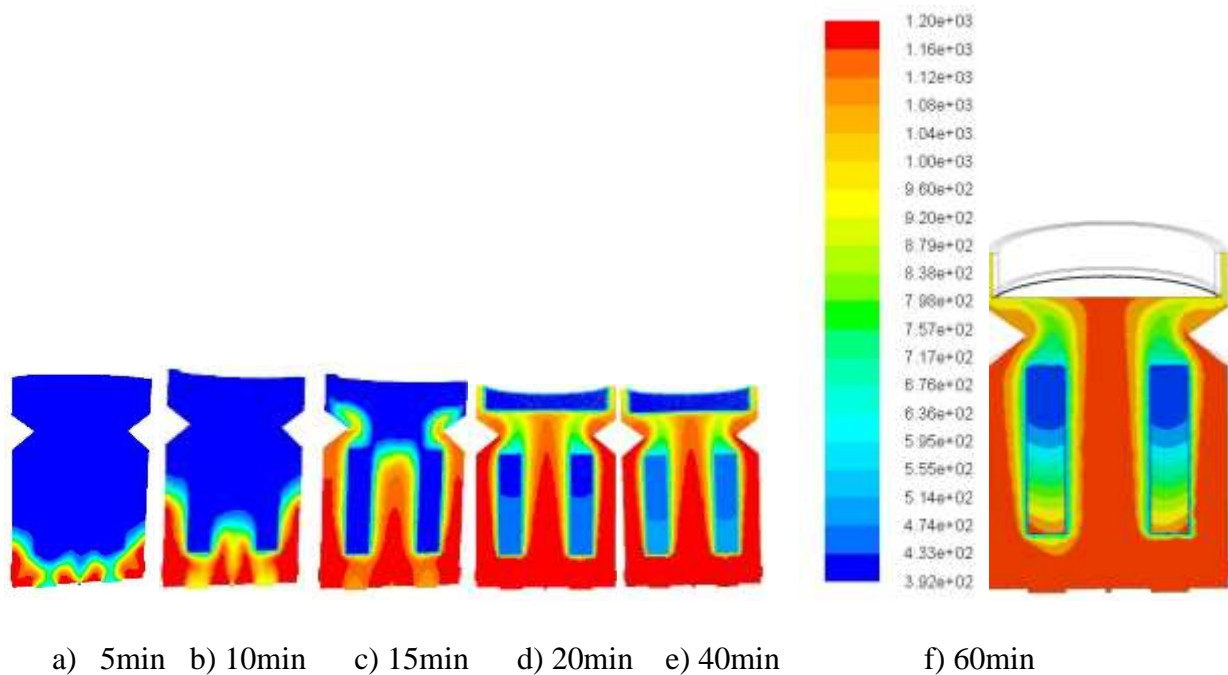


Figure 12: Transient heat transfer throughout the stove at different time from bottom to top

Figure 13 shows the transient heat transfer from the combustion chamber to the cooking pot at different time. As time increases the temperature through the stove increases

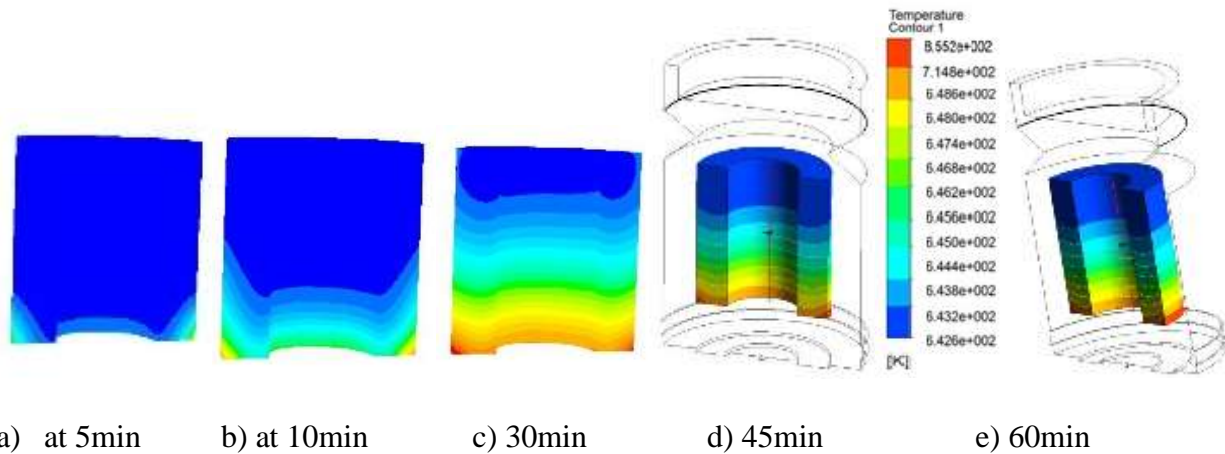


Figure 13: Transient heat transfer through the biomass to be charred

Figure 15 shows the heat transfer from combustion chamber to biomass bed. Similar with the above one as combustion time increase, the temperature transfer through the biomass to be charred is also increased. The result shows that the heat is transferred from bottom to top and from inner and outer to the mid-point.

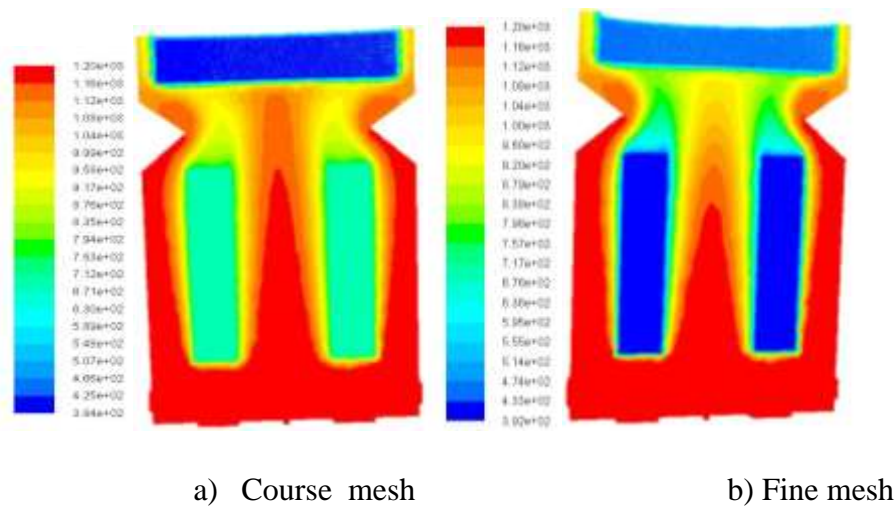
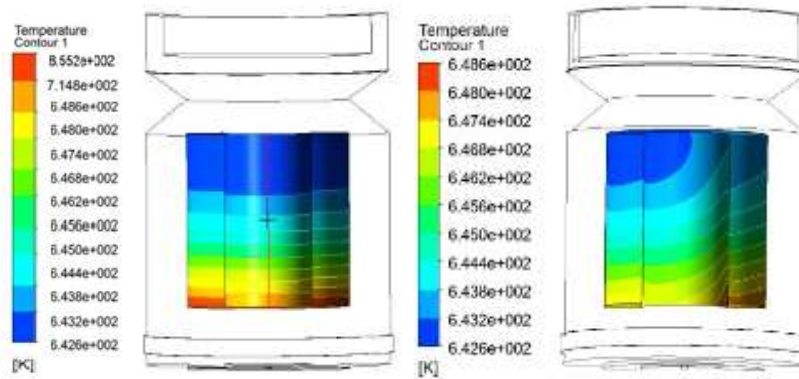


Figure 14: Effect of mesh size

The figure 16 shows the temperature of the coarse mesh is less than the temperature of fine mesh in fluid domain and vice versa in solid domain at a given time.



a) Air supplied only from bottom direction b) Air supplied from bottom and side direction

Figure 15: Effect of primary air flow direction

Figure 17 shows the effect of air inlet direction. The result indicates the direction of air supplied is an important issue. If air is supplied from side flame enforced to leave the center of the stove, but if the air is supplied fully only from bottom the flame is distributed equally through the the stove and the heat is transferred properly.

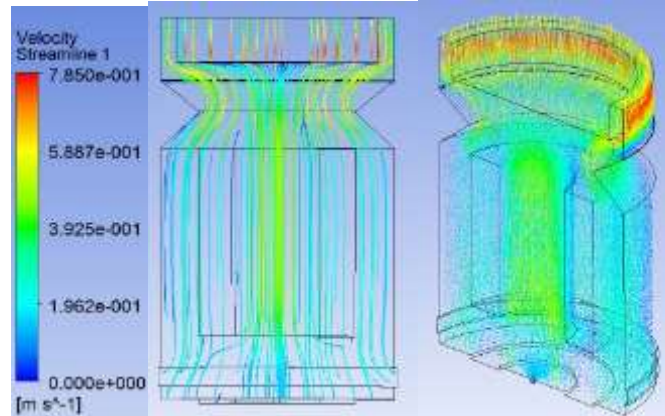


Figure 16: Flow velocity in the combustion chamber of stove

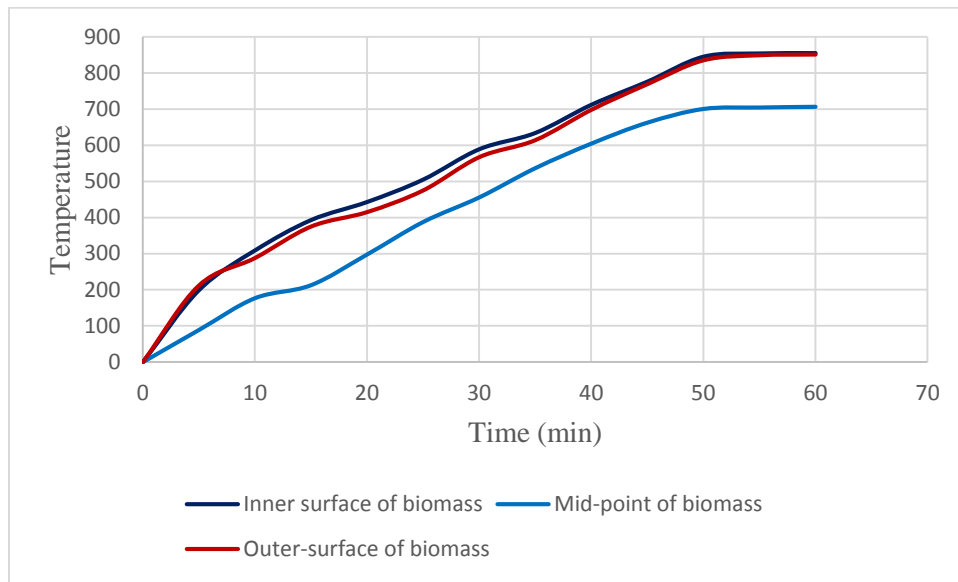


Figure 17: trend of Temperature with time in coffee husk at selected point

Figure 19 shows the variation of CFD simulation Temperature with time. As time increase the temperature also increase at the inner, mid-point and outer surface respectively. At 60min the temperature of the three selected points reached the range of biochar temperature (300°C to 600°C). The temperature of inner and outer surface of biomass is greater than the temperature of mid-point biomass because of the heat which is supplied from the inner and outer cylinder.

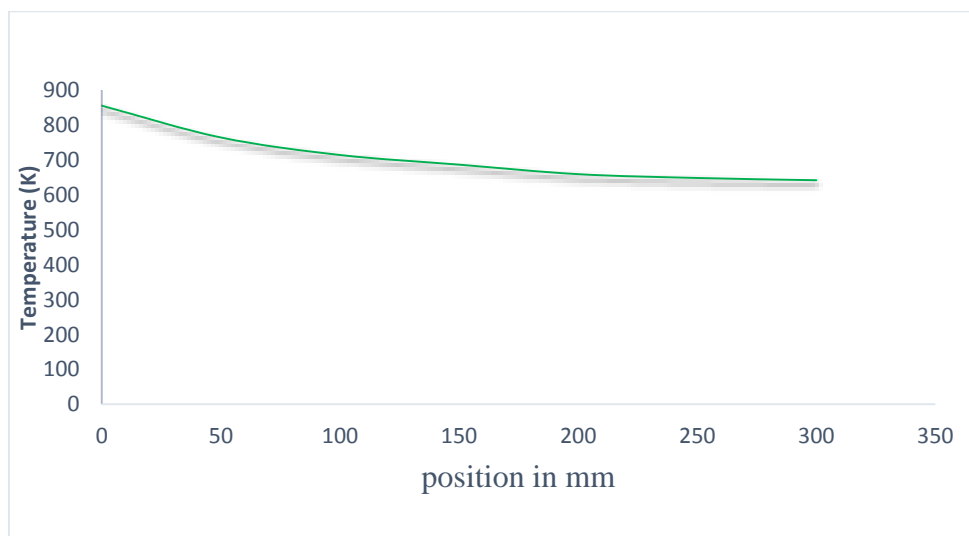


Figure 18: Heat transfer throughout the biochar from bottom to top at (45min)

Figure 20 shows that the temperature variation with position from bottom to top. The temperature varies 855K to 642K from bottom to top. The result shows the temperature variation within biomass is less.

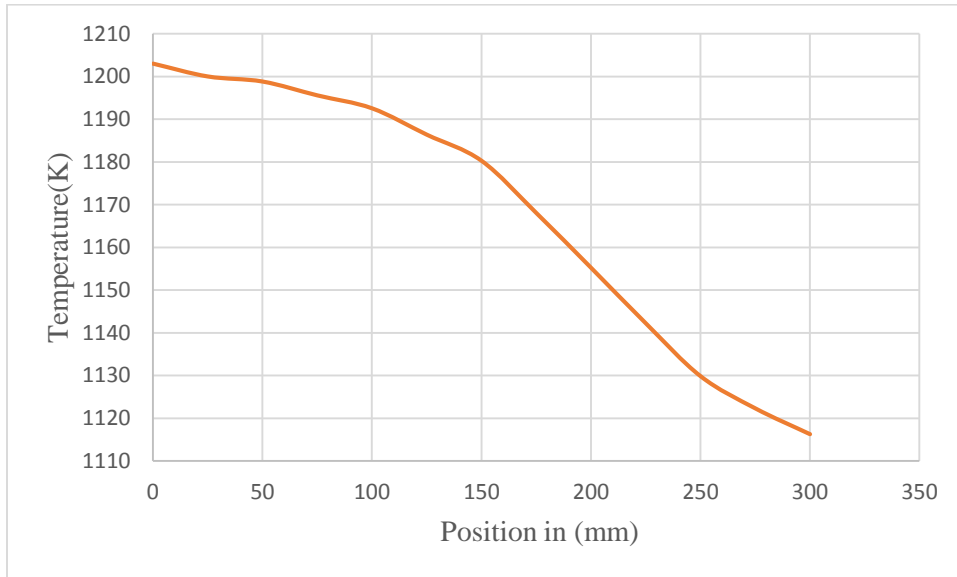


Figure 19: Temperature variation throughout the stove at 45min from bottom to top

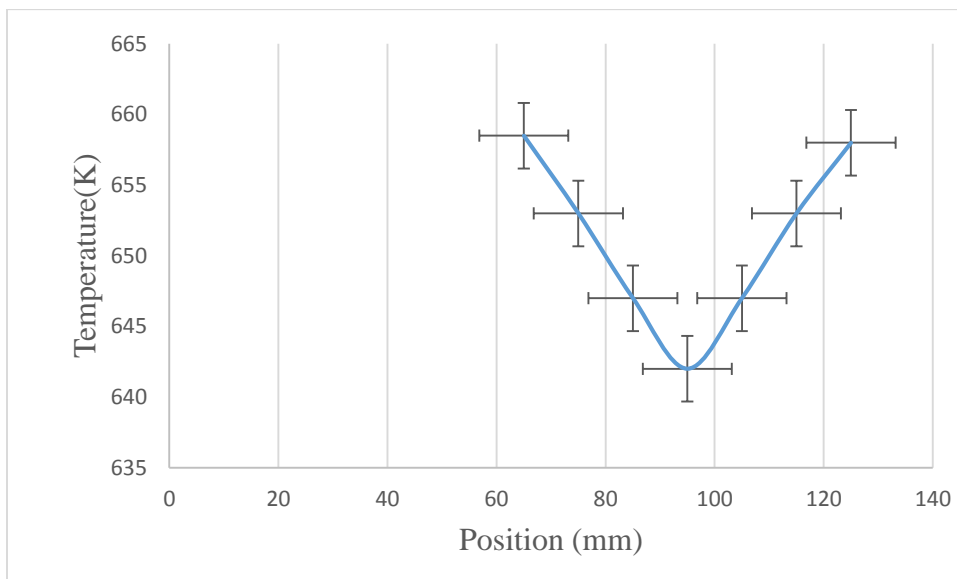


Figure 20: CFD results of temperature variations within biomass to be charred at selected line from inner to outer at 45min

Figure 22 shows the temperature variation with position within biomass to be charred. The temperature is decreased from inner surface biomass temperature of 658K to mid-point biomass temperature of 642K and it starts increase to 657.5 at outer surface of biomass.

4.2 Results from experimental validations

The experimental results are discussed in the following one by one, such as Water boiling test, trend of temperature within biomass to be charred with position and time

4.2.1 Water boiling test

The WTB is one method which is used throughout the world to test the performance of stoves. In this study WBT version 4.2.2 is used and it is simple test to collect data's.

4.2.1.1 Effect of angle of cone and secondary air



a) without secondary air b) with high inlet of secondary air c) with low inlet of secondary air

Figure 21: experimental results which shows the effect of secondary air inlet

4.2.1.2 Measured biochar temperature variations during water WBT

Figure 24 shows the temperature variation with time within biomass bed at inner surface, mid-point, and outer surface of biomass bed. In all stoves the temperature trend is similar, but the values are different from one to each other.

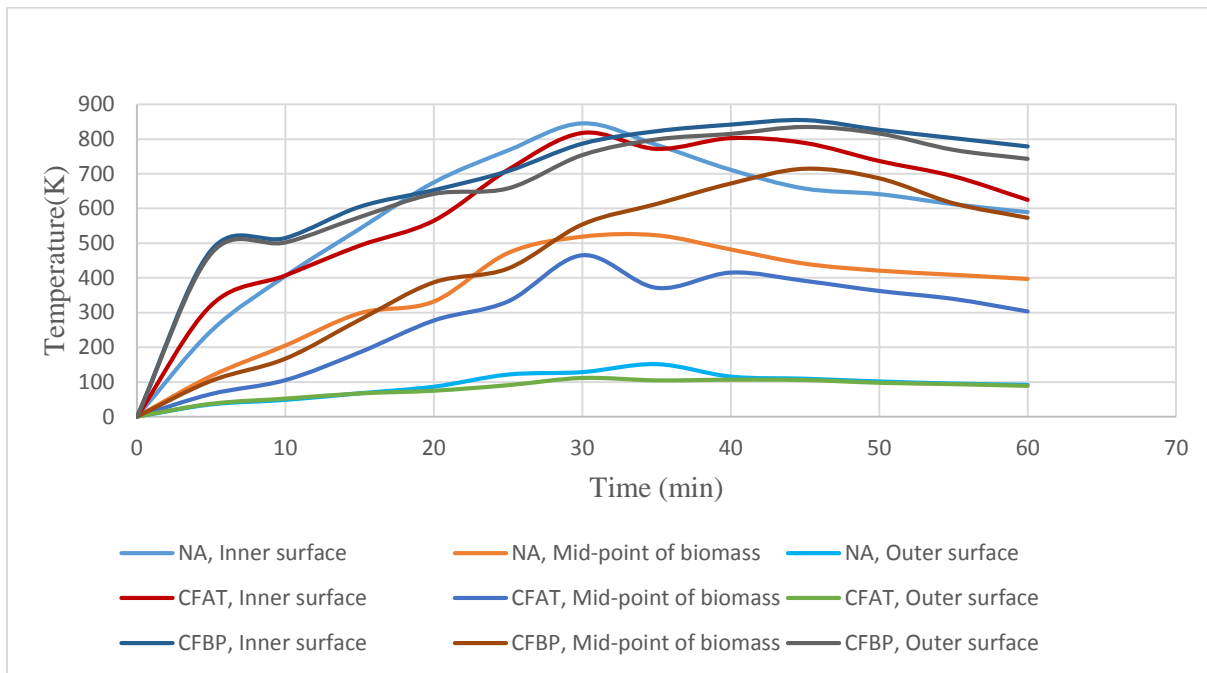


Figure 22: Temperature versus time at different position within biomass for selected stoves

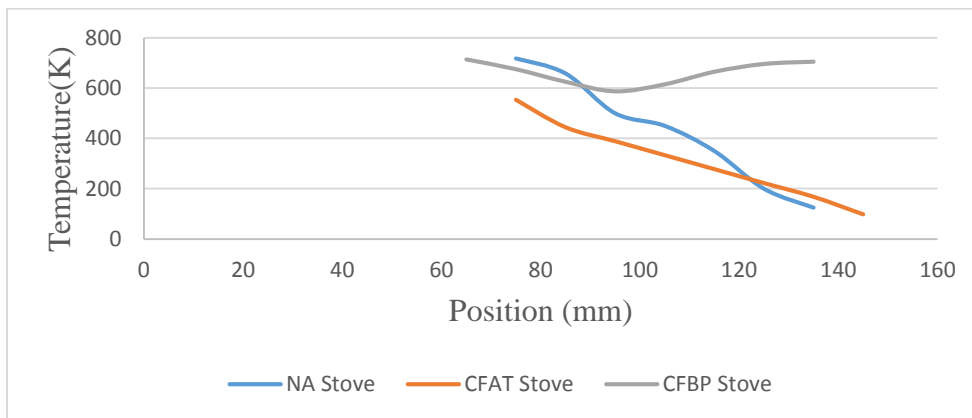


Figure 23: Experimental Temperature variations with position for selected stoves at 60min

The experimental temperature trend with position at 60min in NA stove and CFAT stove was decreased. Similar with CFD simulation, experimental results shows the temperature variation within biomass bed is high in both NA and CFAT stoves while it is small temperature variation in CFBP stove.

4.2.1.3 Time to cook.

The time of the cooking process shows that the continuous feeding biochar producing stove is slightly faster to use than the normal Anila stove and the continuous feeding Anila type stove (Figure 8). What is also shown in the graph is that the lighting time has a considerable impact on the time of the cooking process. What is also shown from the test results is that the need of reloading the continuous feeding biochar producing stove has an important impact on the cooking time

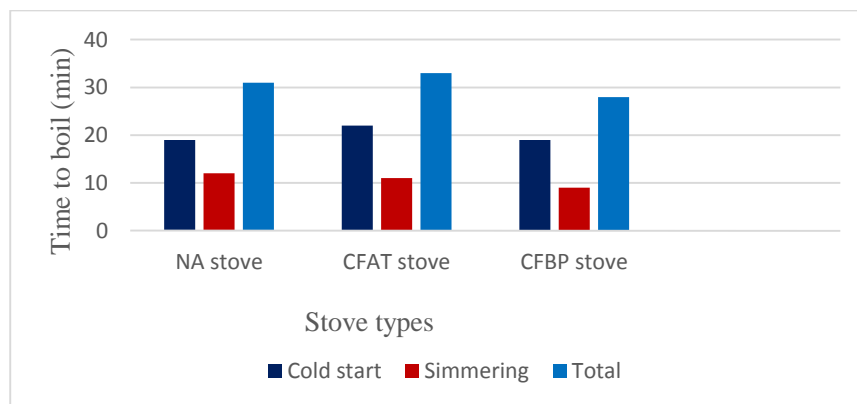


Figure 24: Average time of cooking processes

4.2.1.4 Fuel consumption

The mean values of fuel consumption during water boiling test are shown below in Figure 11.

The results of the tests shows that the continuous feeding biochar producing stove has the lowest fuel consumption, followed by the normal Anila stove and the continuous feeding Anila type stove.

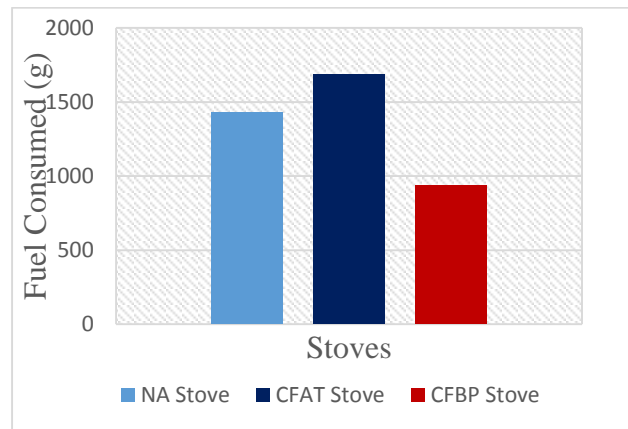


Figure 25: Average fuel consumption for all stove

4.2.1.5 Thermal efficiency of stoves

Thermal efficiency was performed on the three stoves using eucalyptus tree as a fuel. It was observed that the CFBP cook stove, CFAT stove and NA stove shows a thermal efficiency of 25%, 18%, and 17% in the case of high power test (cold start). And also the thermal efficiency of CFBP stove, CFAT stove and NA stove shows 15%, 13%, and 13% in the case of low power test (simmering) Thus, it was found that the thermal efficiency of CFBP cook stove is found to be higher when compared with the other two stoves in both cases. Results of thermal efficiency showed in Fig 28.

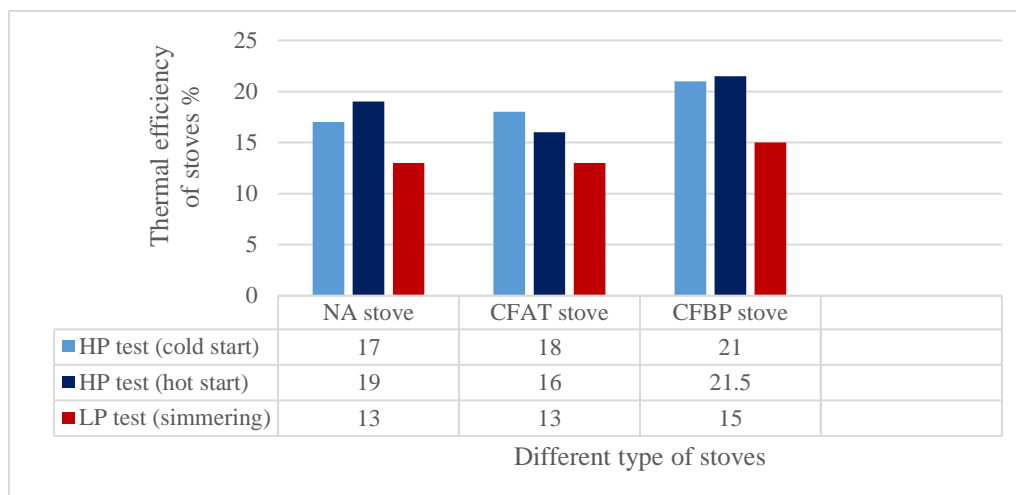


Figure 26: Thermal efficiency of the three stoves in the case of high power and low power test

4.2.1.5 Firepower

The firepower is a measure of the heat output of the stoves and the turn-down ratio is an indicator of the control range of fire the power. The higher the turn-down ratio, the greater the power control ranges of the stove. In the cold and hot start phases, the continuous feeding biochar producing cookstove had the highest firepower while it had the lowest firepower for the simmer phase. Due to this, the continuous feeding biochar producing cookstove had the highest turn-down ratio of 2.8.

The Normal Anila stove had the second highest turn-down ratio of 2.21 followed by the Continuous feeding Anila type stove with a turn-down ratio of 1.78. It had the lowest firepower during both the cold start and hot start phases and the highest firepower during the simmer phase. Figure 29 and 30 shows the graphical representation for the comparison of the firepower of the stoves in each of the water boiling test phases and the corresponding turn-down ratio, respectively.

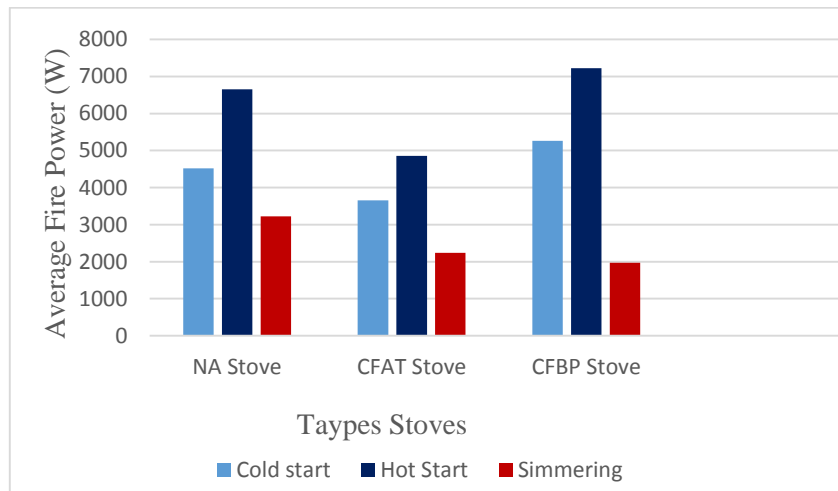


Figure 27: Comparison of the power of the each stoves

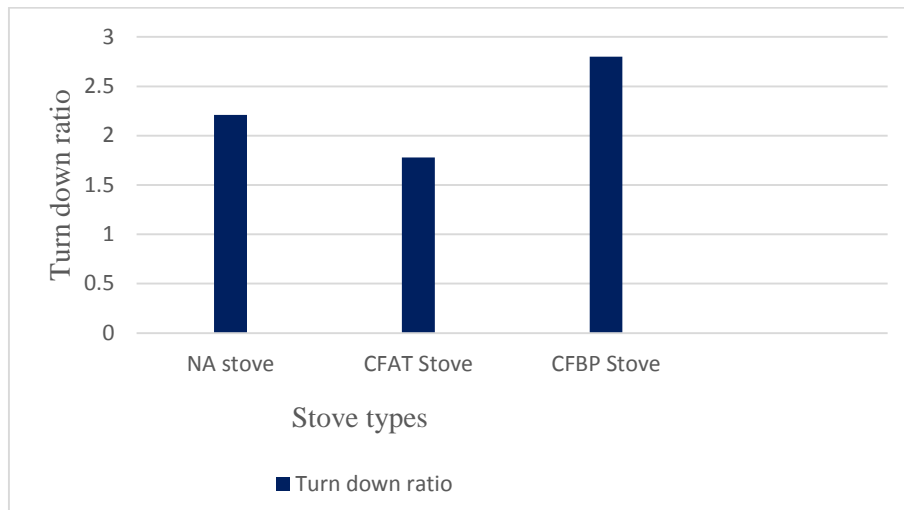


Figure 28: Comparison of turn down ratio of each stoves

4.2.2 Produced Biochar and its characterizations

4.2.2.1 Produced Biochar

The biochar is produced by the three selected stoves to compare the performance of the new stove during water boiling test. First the new stove was done according to the result of CFD simulation. During WBT at 60min the coffee husk temperature gained was much with the CFD simulation temperature (642K to 855K) which is enough to changed coffee husk to biochar. The two left stoves also used up to 60min to evaluate the biochar produced from the stoves at constant time. As the results of figure 31 below shows biochar is not produced at one round of cooking.



a) Normal Anila stove



b) CA stove



c) CBPN stove

Figure 29: the biochar produced from the three types of stove

4.2.2.2 Physico-chemical characteristics of biochars

Coffee husk biochar was initially sieved through sieves of different sizes (1,000, 710, 500, 355, and 250, 180 and 125 mm) in order to determine the particle size distribution of the biochar. For biochar moisture, volatile matter and ash contents determination, a modified version [23] of ASTM (American society for Testing and Materials) method D1762-84 was used. The heating rate values correspond to the heating rate of coffee husk during the pyrolysis process for biochar production at 300°C, 450°C and 600°C, respectively and were calculated by considering the ramping time (1 h) needed to reach those target temperatures.

Table 4: Proximate analysis of biochar gained from selected biomass

Properties	Coffee husk		
	Samples at different temperature (°C)		
	300 (°C)	450 (°C)	600 (°C)
Moisture (%)	1.87	2.93	3.12
Volatile matter (%)	47.12	25.32	15.05
Ash (%)	2.53	3.52	5.35
Fixed carbon (%)	48.25	69.63	81.5

4.2.2.3 Conversion of biomass to biochar

As time increase the heat transferred within biomass is increased and it causes biomass mass loss was increased. At 60min the coffee husk mass is lost by 73.2%.

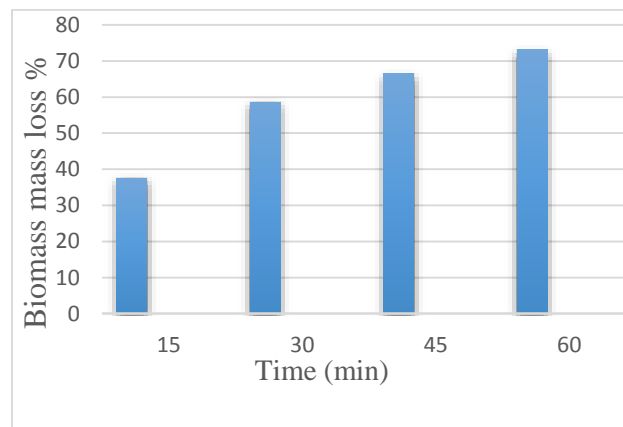


Figure 30: Coffee husk mass loss (%) to biochar versus time (min)

4.2.2.4 Yield of biochar from biomass

The bar graph below shows the percentage of biochar that was produced from each set of conditions. As temperature increased the percentage yield of biochar produced is also increased.

The biochar yield at 600K is 25.17% wt while at 300K is 45.25% wt

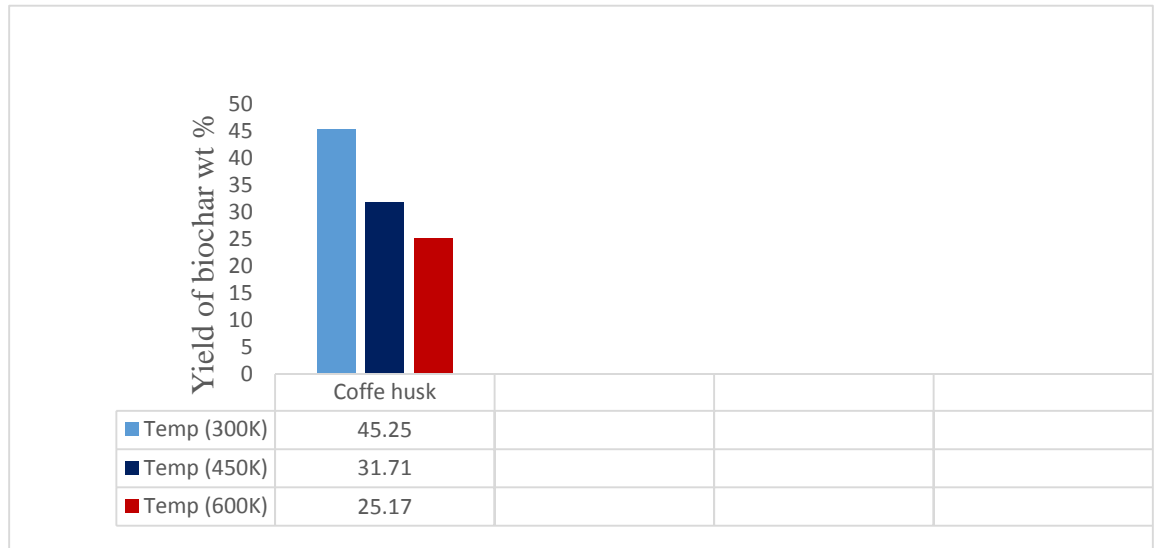


Figure 31: Biochar yield of selected biomass at different temperature (K)

From the graph evident correlations can be made due to the temperatures and the initial states of the biomass. Temperature played a major role in the yield. As the temperature was increased for each sample, the yield decreased. This is due to the obvious correlation that with exposure to extreme temperature conditions the biomass will be diminished faster than normal. At 300°C coffee husk had the highest remaining yield; this may correlate with the initial conditions/form of the biomass.

4.2.2.5 Surface Area of biochar produced

. Having a high surface area is important to the placement of the biochar underground. With larger surface area per gram of a sample there is less erosion and more ability to capture any particulates that may pass through the sink or into the biochar fertilized soil. Therefore the longevity is increased and carbon capturing can take place over a longer period of time. Figure 34 shows, the higher temperatures have the larger surface area and saw-dust has the larger square meter per gram. Similar to previous characterization, this can be connection to the initial sample of biomass that was used and also the grinding method that was used for preparation prior to the testing.

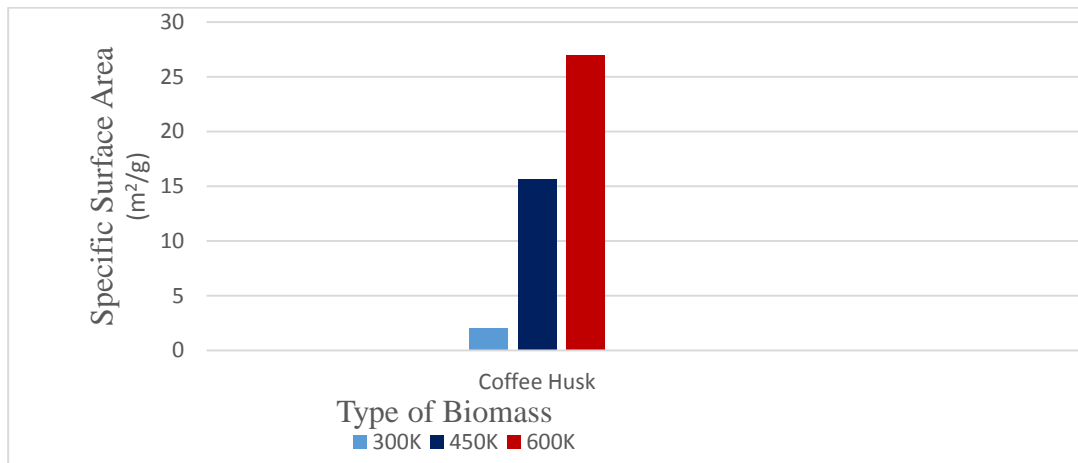


Figure 32: surface area of biochar produced in new stove at different temperature

4.2.2.6 Biochar pH

The biochar produced is highly alkaline, with all pH values recorded above pH 9.33 to a maximum pH of 9.63. The variability within the sample chosen from each burn is low, which means that coffee husk biochar produced experimentally is consistent in terms of pH with in a given burn.

Table 5: pH of biochar produced of continues feeding biochar producing cook stove by experiments

Stove Type	Biochar (g)	pH(1)	pH(2)	pH(3)	Average
NA Stove	180	9.33	9.33	9.27	9.33
CFAT Stove	205.5	9.57	9.55	9.63	9.58
CFBP Stove	175	9.62	9.43	9.44	9.63

4.3 Comparison of CFD simulation results and Experimental data

Comparison of CFD result with experimental result was an essential to evaluate the produced stove performance. The two figure below shows the temperature variation with time and position

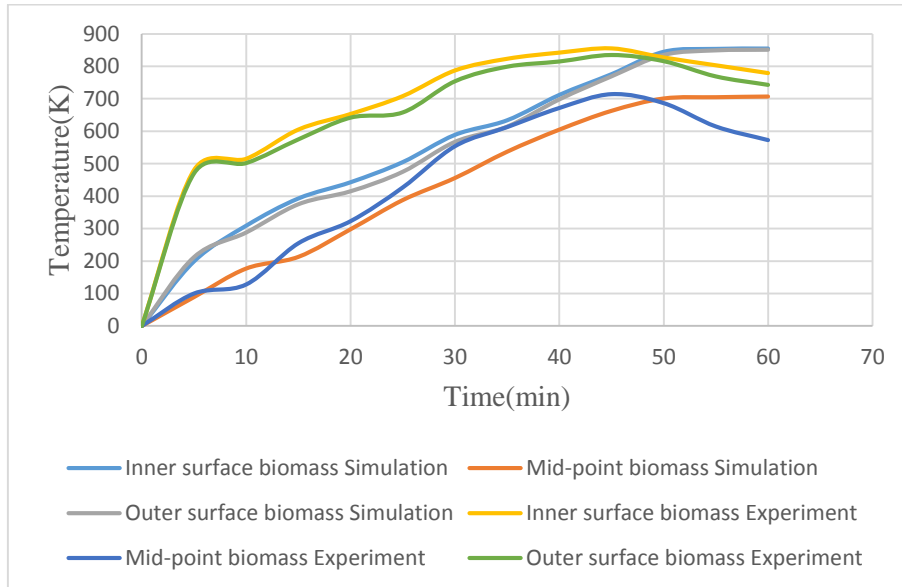


Figure 33: Experimental and CFD simulation result of temperature variation with time for selected point

Figure 36 shows the experimental and CFD simulation of Temperature variation with time. As figure shows the overall result of CFD simulation Temperature is less than experimental temperature results up to 50min and vice versa from 50min to 60min. When compared with simulation result there is a large gap between inner and outer surface of biomass temperature experiment and mid-point biomass temperature experiment because of the size of wood fuel which is difficult to inject fully the bottom of the stove. The result of temperature gained is satisfactory in both CFD simulation and Experimental results to produce qualified biochar while cooking.

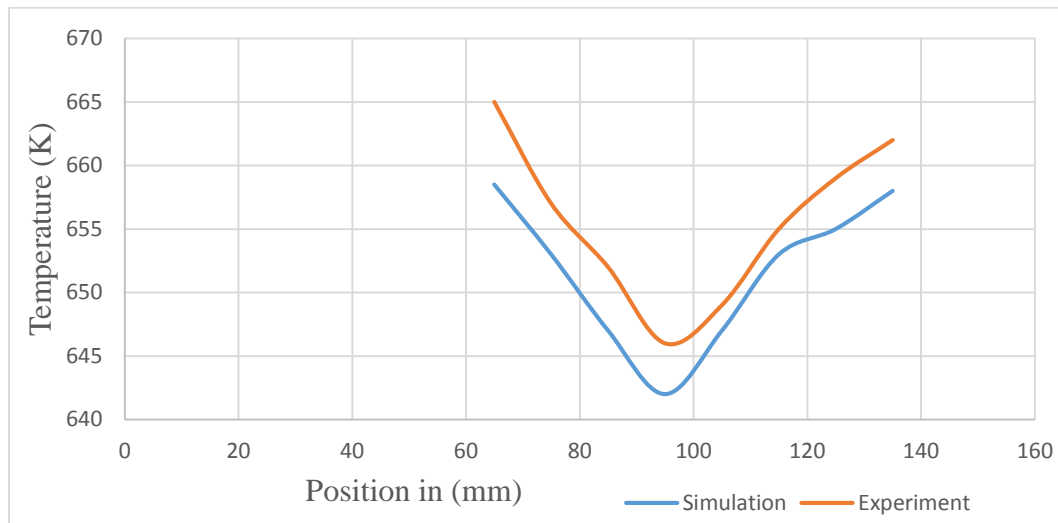


Figure 34: Experimental and Simulation result of Temperature variation with position

Figure 36 shows the experimental and simulation of temperature variation with position. The temperature of experimental result is higher than the CFD simulation temperature, But the temperature variation with in biomass (coffee husk) between CFD simulation and Experimental result is very small which is varied from 665, 646 and 662(K) at inner, mid-point and outer surface of biomass respectively for Experimental results and varies from 658, 642 and 658(K) at inner, mid-point, and outer surface of biomass.

CONCLUSION AND RECOMMENDATION

Conclusion

Overall, approximately 45 cases were studied during the development of this model. The majority of these cases were run to gain an understanding of how various parameters affected the solution.

This paper summarized the CFD applications in biomass combustion and system design. There is evident that CFD can be used as a powerful tool to predict biomass combustion and heat transfer processes as well as to design combustion chamber or reactor. CFD has played an active part in system design including analysis the flow, and temperature. The CFD model results are satisfactory and have made good agreements with the experimental data in many cases. However, the simulations still have many approximate models as well as some assumptions. To ensure CFD simulations are more than just theoretical exercises, experimental validation is necessary to facilitate the model accuracy. With the progressing of the computing power and the development of chemical and physical models, the CFD applications in the biomass combustion will more widely spread in the future

During the course of this research project, realistic geometry, flow conditions, and fuel properties were incorporated into a 3D numerical model using Fluent CFD software (ANSYS 14.5). By performing simulations with different direction of air inlet and mesh size, it was shown that the 3D model performed fairly well, and exhibited the expected trends for temperature, and flow of syngas. Similar with CFD simulation, experimental results shows the temperature variation within biomass bed is high in both NA and CFAT stoves while it is small temperature variation in CFBP stove.

It was observed that the CFBP cook stove, CFAT stove and NA stove shows a thermal efficiency of 25%, 18%, and 17% in the case of high power test (cold start). And also the thermal efficiency of CFBP stove, CFAT stove and NA stove shows 15%, 13%, and 13% in the case of low power test (simmering) Thus, it was found that the thermal efficiency of CFBP cook stove is found to be higher when compared with the other two stoves in both cases.

The biochar produced is highly alkaline, with all pH values recorded above pH 9.33 to a maximum pH of 9.63. The variability within the sample chosen from each burn is low, which means that coffee husk biochar produced experimentally is consistent in terms of pH with in a given burn.

Jimma University, Jimma institute of Technology, Faculty of Mechanical Engineering, Sustainable Energy Engineering program

Recommendations

Based on the results, discussion, and conclusions found in this report, the following actions are recommended:

It is recommended that more instrumentation be installed on the stove:

- Multiple temperature sensors should be installed to give an accurate representation of the temperature distribution throughout the chamber. These sensors should be placed at varying vertical and horizontal heights
- A method of measuring the air entering the primary chamber through the fuel port should be devised.
- As well, enough instrumentation must be installed to determine whether air is introduced to the pyrolysis system at other locations.
- The amount of ash produced during each run should be recorded to give a proper mass balance.

The particulate matter and Gas emissions to be tested. The inner holes used to collect syngas from pyrolysis chamber must be carefully designed. This technology can be sustained using local available resources such as fuel and manpower for day-to-day operation of the technology.

Due to the shortage of money, time and logistics, kitchen performance test and control cooking test (CCT) has not been carried out. Only WBT were carried out. After conducting the two tests, kitchen performance test should have been carried out in order to assess the fuel efficiency of the stove under normal condition. Thus it is recommended that the test should be conducted in order to get the real performance of the stove in fuel saving, even though it requires longer time and high investment.

From experimental results it has been observed that the average thermal efficiency of this continuous feeding biochar producing stove is about 25%. These efficiencies are very low as compared to modern stoves such as kerosene stoves and electric stove. Therefore, it needs to do further work to improve the efficiency of the stove to safeguard the environment and improve the wellbeing of the people.

Additional testing should also be conducted in the field. The Water Boiling Test and other

laboratory based performance evaluations are not adequate representations of stove operation and cooking practices in real world settings. The qualitative survey portion of the Kitchen Performance Test (KPT) was used in this study to solicit user feedback. The full test also includes a quantitative measure of household fuel use over a prescribed period of time both before and after stove implementation. The Kitchen Performance Test provides a real world assessment of a stove's efficiency while gaining valuable user feedback.

Bibliography

- [1] I. Evaluation, I. C. Stoves, and B. Faso, "Impact Evaluation of Improved Cooking Stoves in Burkina Faso IOB Evaluation Impact Evaluation of Improved Cooking Stoves in Burkina Faso," no. 388.
- [2] "CLEAN FUEL-SAVING TECHNOLOGY ADOPTION IN URBAN ETHIOPIA 1 Abebe Damte Beyene 2 and Steven F. Koch 3," vol. 27, no. 12, pp. 1–24.
- [3] S. Cookstoves, "Affordable Biochar Production Options," no. June, 2013.
- [4] D. Amare, A. Endebhathu, and A. Muhabaw, "Enhancing Biomass Energy Efficiency in Rural Households of Ethiopia," vol. 4, no. 2, pp. 27–33, 2015.
- [5] S. H. Kooser, "Clean Cooking : The Value of Clean Cookstoves in Ethiopia Clean Cooking : The Value of Clean Cookstoves in Ethiopia," vol. 01, no. 01, 2014.
- [6] M. Teferra, "Energy and economic growth in ethiopia," pp. 197–209, 1986.
- [7] I. The, S. Development, E. Poverty, S. Africa, E. Electric, P. Corporation, and S. African, "Study on the Energy Sector in Ethiopia," pp. 1–16, 2008.
- [8] M. C. Stove, "List of Stoves in Ethiopia Improved Household Injera Baking Stoves."
- [9] G. T. Tucho and S. Nonhebel, "Bio-Wastes as an Alternative Household Cooking Energy Source in Ethiopia," pp. 9565–9583, 2015.
- [10] E. Adkins, J. Chen, J. Winiacki, P. Koinei, and V. Modi, "Energy for Sustainable Development Testing institutional biomass cookstoves in rural Kenyan schools for the Millennium Villages Project," 2010.
- [11] "University of Oldenburg / Germany Efficiency test for a biomass cooking stove."
- [12] Z. Gebreegziabher, "LAND DEGRADATION IN ETHIOPIA : WHAT DO STOVES HAVE TO DO WITH IT ?," 2006.
- [13] U. N. Foundation, B. Air, and M. Group, "Stove Performance Inventory Report Prepared for the Global Alliance for Clean Cookstoves United Nations Foundation Berkeley Air Monitoring Group," no. October, 2012.
- [14] A. R. Effects and M. Logit, "Environment for Development Household Fuel Choice in," no. October, 2013.

- [15] V. Clarke, “The Pyrolytic Stove Cooking Smoke Inhalation :,” vol. 000, pp. 1–4, 2011.
- [16] A. U. Thesis, “Development of Efficient and Cleaner Charcoal Stoves for Cooking Applications in a Rural Residential Dwelling,” no. January 2015.
- [17] F. Report, “IMPROVED COOK STOVES,” 2012.
- [18] S. C. Bhattacharya and M. A. Leon, “PROSPECTS FOR BIOMASS GASIFIERS FOR COOKING APPLICATIONS IN ASIA.”
- [19] M. Mensah, “Pyrolysis and Biochar for Soil Enrichment Research areas - 2 nd Generation Biofuels,” no. March, 2012.
- [20] P. S. Anderson, “Increasing Biochar Production with Micro- and Mini- Sized Methods and Devices,” no. August, 2014.
- [21] T. Tomlinson and I. B. Initiative, “2013 State of the Biochar Industry A Survey of Commercial Activity in the Biochar Field,” no. March, 2014.
- [22] R. Andre, G. Defosse, and P. L. E. Parlouër, “Biomass pyrolysis reactions and products as studied by simultaneous thermal analysis techniques,” vol. 86, no. 2007, p. 69300, 2010.
- [23] “Biochar for soil quality improvement, climate change mitigation and more,” pp. 1–45.
- [24] A. Nigussie, E. Kissi, M. Misganaw, and G. Ambaw, “Effect of Biochar Application on Soil Properties and Nutrient Uptake of Lettuces (*Lactuca sativa*) Grown in Chromium Polluted Soils,” vol. 12, no. 3, pp. 369–376, 2012.
- [25] T. T. Mengesha and A. V. Ramayya, “Heat Transfer Validation and Comparative Evaluation of Biochar Yield from Pyrolysis Cook Stove,” vol. 5, pp. 389–400, 2015.
- [26] J. I. Network, W. P. Van Der Gaast, and E. Spijker, “Biochar and the Carbon Market,” no. November, 2013.
- [27] P. Objective and P. Highlights, “Piloting Pyrolytic Cook Stoves and Sustainable Biochar Soil Enrichment in Northern Vietnam Uplands Relevance to Country ’ s Energy and Environment Piloting Pyrolytic Cook Stoves and Sustainable Biochar Soil Enrichment in Northern Vietnam Uplands.”
- [28] D. Centre and S. Carter, “Workshop on Biochar - Production and Uses Organised by the UK Biochar Research Centre , University of Edinburgh Thursday 16 th - Friday 17 th September 2010,” no. September, pp. 1–17, 2010.

- [29] O. G. G. Knox, C. O. Oghoro, F. J. Burnett, and J. M. Fountaine, "BIOCHAR INCREASES SOIL pH , BUT IS AS INEFFECTIVE AS LIMING AT CONTROLLING CLUBROOT," vol. 97, pp. 149–152, 2015.
- [30] A. K. Sharma, M. R. Ravi, and S. Kohli, "MODELLING PRODUCT COMPOSITION IN SLOW PYROLYSIS OF WOOD."
- [31] E. Benefits, F. Biochar, C. In, and T. H. E. Central, "BIOCHAR CLUSTER," no. May, pp. 1–35, 2014.
- [32] T. Brandstaka, J. Helenius, J. Hovi, A. Simojoki, H. Soenne, and P. Tammeorg, "Biochar filter : use of biochar in agriculture as soil conditioner," no. December, pp. 1–22, 2010.
- [33] A. K. Berek, N. Hue, and A. Ahmad, "Beneficial Use of Biochar To Correct Soil Acidity," no. November, pp. 3–5, 2011.
- [34] A. Mukherjee, A. R. Zimmerman, R. Hamdan, and W. T. Cooper, "Physicochemical changes in pyrogenic organic matter (biochar) after 15 months of field aging," pp. 693–704, 2014.
- [35] F. Report, *Use of Biochar from the Pyrolysis of Waste Organic Material as a Soil Amendment Ecology Publication Number 09-07-062*. 2009.
- [36] F. L. Article, "Effect of Biochar on pH of Alkaline Soils in the Loess Plateau : Results from Incubation Experiments," no. 2010, pp. 745–750, 2012.
- [37] A. Abewa, B. Yitafaru, Y. G. Selassie, and T. Amare, "The Role of Biochar on Acid Soil Reclamation and Yield of Teff (*Eragrostis tef* [Zucc] Trotter) in Northwestern Ethiopia," vol. 6, no. 1, pp. 1–12, 2014.
- [38] D. A. Laird, "Chapter 16 Pyrolysis and Biochar-Opportunities for Distributed Production and Soil Quality Enhancement," no. Figure 1, pp. 257–281, 2010.
- [39] S. Carter, S. Shackley, S. Sohi, T. B. Suy, and S. Haefele, "The Impact of Biochar Application on Soil Properties and Plant Growth of Pot Grown Lettuce (*Lactuca sativa*) and Cabbage (*Brassica chinensis*)," pp. 404–418, 2013.
- [40] R. W. Larson, "Using Biochar for Sequestration in Soils," 2007.
- [41] E. P. Number, *Methods for Producing Biochar and Advanced Biofuels in Washington State Part 1 : Literature Review of Pyrolysis Reactors*, no. April. 2011.
- [42] T. Exhibition, "COMBUSTION EFFICIENCY IN BIOMASS FURNACES WITH FLUE GAS CONDENSATION," 1998.

- [43] “BIOCHAR PRODUCTION WITH COOK STOVES AND USE AS A SOIL,” no. January, 2011.
- [44] R. C. Brown, “Biochar Production Technology.”
- [45] M. Abberton, “Grassland carbon sequestration : management , Proceedings of the Workshop sequestration in the mitigation of.”
- [46] J. Jetter, Y. Zhao, K. R. Smith, B. Khan, T. Yelverton, P. Decarlo, and M. D. Hays, “Pollutant Emissions and Energy Efficiency under Controlled Conditions for Household Biomass Cookstoves and Implications for Metrics Useful in Setting International Test Standards Pollutant Emissions and Energy Efficiency under Controlled Conditions for Household Biomass Cookstoves and Implications for Metrics Useful in Setting International Test Standards,” 2012.
- [47] B. Production, T. H. E. Peko, and P. E. Stove, “Project report,” 2011.
- [48] J. Tryner, A. J. Marchese, and B. D. Willson, “The Effects of Fuel Type and Geometry on Emissions and Efficiency of Natural Draft Semi-Gasifier Biomass Cookstoves,” 2013.
- [49] D. Gesellschaft and I. Zusammenarbeit, “International Agricultural Research List of BMZ Funded Projects,” no. August, 2015.
- [50] C. R. Lohri, D. Sweeney, and H. M. Rajabu, “CARBONIZING URBAN BIOWASTE FOR LOW-COST CHAR PRODUCTION IN DEVELOPING COUNTRIES A Review of Knowledge , Practices and Technologies.”
- [51] D. F. Fletcher and S. D. Joseph, “A CFD based combustion model of an entrained flow biomass gasifier,” vol. 24, no. 2000, pp. 165–182, 2006.
- [52] S. Zahirovic, R. Scharler, and I. Obernberger, “Advanced CFD modelling of pulverised biomass combustion.”
- [53] R. Chodapaneedi, N. Sanke, and D. N. Reddy, “CFD Simulation of an Advanced Biomass Gasifier,” pp. 42–48.
- [54] S. Carter and S. Shackley, “Biochar Stoves : an innovation studies perspective,” no. April, 2011.
- [55] I. F. Training, “Heat Transfer Modeling,” 2006.
- [56] “Main reactions during biomass gasification Primary devolatilization Primary tar (CH₄,” p. 14.

- [57] S. Money, “WOOD BURNING HANDBOOK Protecting the Environment.”
- [58] M. A. Muilenburg, “Computational modeling of the combustion and gasification zones in a downdraft gasifier,” 2011.
- [59] C. Emissions, “The Water Boiling Test,” vol. 2, no. January 2013, 2014.

APPENDIXES

CFD Simulation result of temperature versus position of new stove

Position	Inner surface of biomass	Mid-point of biomass	Outer surface of biomass
0	0	0	0
5	199	89	212
10	309	177	288
15	393	213	375
20	443	298	415
25	505	388	475
30	589	456	567
35	634	537	614
40	712	605	698
45	776	663	769
50	845	701	835
55	854	705	849
60	855	707	851

WATER BOILING TEST PROCEDURES

The procedures used in the stove test were based on the water boiling test protocol 4.2.3 (Global Alliances for Clean Cookstoves 2014).

Cold Start Phase

The following were the procedures used for the cold start phase:

1. Weigh the pot, ash tray and the stove.
2. Weigh the amount of charcoal to be used.
3. Weigh the stove loaded with charcoal.
4. Weigh the pot with initial amount of water

5. Place the pot on the stove. Using the pot lid with drilled hole to hold the thermometer, measure the temperature approximately 2.5 cm above the center. Measure the initial water temperature in the pot (shown in figure 1).
6. Start the fire in a reproducible manner according to local practices. In this test, kerosene was used as the fire starter (shown in figure 2). The ignition procedure was done outside the test area.
7. Once the fire has caught, weigh the stove with the fuel again. Start the timer and record the starting time. Bring the first pot rapidly to a boil without being excessively wasteful of charcoal. Control the fire with the means commonly used locally. For this test, a hand fan was used to control the fire. Also, every 15 minutes, additional 40 g of charcoal was added in the stove. Figure 3 shows the prepared 40 g of charcoal for fuel addition.
8. When the water in the first pot reaches the pre-determined local boiling temperature as shown by the thermometer, rapidly do the following steps:
 - ✓ Record the time at which the water in the primary pot first reaches the local boiling temperature.
 - ✓ Carefully separate the remaining charcoal and the ash. Weigh them separately
 - ✓ Weigh the pot with its remaining water
 - ✓ Discard the hot water.

Hot Start Phase

After the cold start, immediately begin the hot start phase. The following were the procedures used for hot start phase:

1. Reset the timer (do not start it yet).
2. Used the previously prepared pot with water that has been weighed.
3. Weigh the stove loaded with fuel.
4. Place the pot on the stove. Measure the initial water temperature in the pot.
5. Start the fire using the fuel from the second pre-weighed bundle designated for this phase of the test. Follow the ignition procedure used in the cold start phase.

6. Once the fire has caught, weight the stove with fuel again. Start the timer and record the starting time. Bring the first pot rapidly to a boil without being excessively wasteful of fuel. Control the fire using the procedure used in cold start phase.

7. When the water in the pot reaches the pre-determined local boiling temperature as shown by the thermometer, rapidly do the following steps:

- ✓ Record the time at which the water in the primary pot first reaches the local boiling temperature.
- ✓ Carefully separate the remaining charcoal and the ash. Weigh them separately.
- ✓ Weigh the pot with its water.

8. Return the remaining charcoal to the stove. Proceed immediately with the simmer phase.

Simmer Phase

The following were the procedures used for simmer test:

1. Reset the timer (do not start it yet).
2. Record the weight of the pot with the remaining water from the hot start.
3. Record the weight of the stove loaded with fuel remaining from the hot start.
4. Relight the charcoal that was replaced.
5. Once the fire has caught, reset and start the timer. Record the starting time.
6. Place the pot on the stove.
7. For 45 minutes maintain the fire at a level that keeps the water temperature as close as possible to 3 degrees below the boiling point. The test is invalid if the temperature in the pot drops more than 6°C below the local boiling temperature. Twenty grams of charcoal was added every time the remaining fuel in the stove is not enough to maintain the temperature.
8. After 45 minutes rapidly do the following steps
 - a. Record the time. Record the final water temperature.

- b. Carefully separate the remaining charcoal and the ash. Weigh them separately.
- c. Weigh the pot with its water.
- d. Discard the hot water.

Results of Water Boiling Test

This section shows all the calculated results for the water boiling test of the improved stoves and the typical stove (see appendix L). Refer to appendix M for the results of the moisture content measurement.

Table 6: Moisture content of three samples of the coffee husk used

Samples	Initial weight(g)	Dry weight	Water(g)	Moisture (%)
1	9.000g	7.53	1.47	15
2	9.000g	7.57	1.43	14
3	9.000g	7.62	1.38	14
Average	-	7.57	1.426	14.33

Table 7: Experimental Temperature trend

Position in(mm)	Temperature								
	NA stove			CFAT Stove			CFBP Stove		
	Inner surface of biomass	Mid-point surface of biomass	Outer surface of biomass	Inner surface of biomass	Mid-point surface of biomass	Outer surface of biomass	Inner surface of biomass	Mid-point surface of biomass	Outer surface of biomass
0	0	0	0	0	0	0	0	0	0
5	247	117	35	321	65	37	480	103	470
10	405	205	48	407	105	52	515	167	502
15	541	298	67	493	185	67	605	279	575
20	675	332	86	565	277	75	653	387	642
25	767	472	121	712	332	91	708	427	658
30	845	519	128	818	465	112	787	554	754
35	783	523	151	772	371	105	823	613	799
40	711	482	115	803	415	107	842	672	815
45	657	441	109	789	391	106	833	714.6	835
50	641	421	101	737	362	98	827	687	816
55	612	409	95	693	339	94	803	615	769
60	589	397	91	625	303	89	779	573	743

Table 8: Summary of the fire power and turn down of each stove during the different water boiling test (WBT) phases.

Stove	Cold start (W)	Hot start (W)	Simmering (W)	Turn-Down Ratio
NA stove	4524	6650	3225	2.21
CFAT Stove	3657	4855	2237	1.78
CFBP Stove	5263	7227	1975	2.8

Table 9: Comparisons of CFD simulation and Experimental data

Time	Simulation			experimental		
	Inner surface biomass Simulation	Mid-point biomass simulation	Outer surface biomass simulation	Inner surface biomass Experiment	Mid-point biomass Experiment	Outer surface biomass Experiment
0	0	0	0	0	0	0
5	199	89	212	480	100	470
10	309	177	288	515	128	502
15	393	213	375	605	255	575
20	443	298	415	653	323	642
25	505	388	475	708	427	658
30	589	456	567	787	554	754
35	634	537	614	823	613	799
40	712	605	698	842	672	815
45	776	663	769	855	714.6	835
50	845	701	835	827	687	816
55	854	705	849	803	615	769
60	855	707	851	779	573	743

Table10: Results of CFD simulation and experimental data temperature vs position

Position	Simulation	Experiment
65	855	805
75	725	675
85	675	625
95	643	587
105	678	625
115	720	665
125	848	750
135	855	755

